Impacts of bromine and iodine chemistry on tropospheric OH and HO2: Comparing observations with box and global model perspectives

Daniel Stone,[1] Tomás Sherwen,[2] Mathew J. Evans,[2,3] Stewart Vaughan,[1] Trevor Ingham,[1,4] Lisa K. Whalley,[1,4] Peter M. Edwards,[2] Katie A. Read,[2,3] James D. Lee,[2,3] Sarah J. Moller,[2,3] Lucy J. Carpenter,[2,3] Alastair C. Lewis,[2,3] Dwayne E. Heard[1,4]

[1] School of Chemistry, University of Leeds, Leeds, UK
[2] Wolfson Atmospheric Chemistry Laboratories, Department of Chemistry, University of York, York, UK
[3] National Centre for Atmospheric Science, University of York, York, UK
[4] National Centre for Atmospheric Science, University of Leeds, Leeds, UK

Abstract

The chemistry of the halogen species bromine and iodine has a range of impacts on tropospheric composition, and can affect oxidising capacity in a number of ways. However, recent studies disagree on the overall sign of the impacts of halogens on the oxidising capacity of the troposphere. We present simulations of OH and HO2 radicals for comparison with observations made in the remote tropical ocean boundary layer during the Seasonal Oxidant Study at the Cape Verde Atmospheric Observatory in 2009. We use both a constrained box model, using detailed chemistry derived from the Master Chemical Mechanism (v3.2), and the three-dimensional global chemistry transport model GEOS-Chem. Both model approaches reproduce the diurnal trends in OH and HO2. Absolute observed concentrations are well reproduced by the box model but are overpredicted by the global model, potentially owing to incomplete consideration of oceanic sourced radical sinks. The two models, however, differ in the impacts of halogen chemistry. In the box model, halogen chemistry acts to increase OH concentrations (by 9.8 % at midday at Cape Verde), while the global model exhibits a small increase in OH at Cape Verde (by 0.6 % at midday) but overall shows a decrease in the global annual mass weighted mean OH of 4.5 %. These differences reflect the variety of timescales through which the halogens impact the chemical system. On short timescales, photolysis of HOBr and HOI, produced by reactions of HO2 with BrO and IO, respectively, increases the OH concentration. On longer timescales, halogen catalysed ozone destruction cycles lead to lower primary production of OH radicals through ozone photolysis, and thus to lower OH concentrations. The global model includes more of the longer timescale responses than the constrained box model and overall the global impact of the longer timescale response (reduced primary production due to lower O_3 concentrations) overwhelms the shorter timescale response (enhanced cycling from HO2 to OH), and thus the global OH concentration decreases. The Earth system contains many such responses on a large range of timescales. This work highlights the care that needs to be taken to understand the full impact of any one process on the system as a whole.

Atmospheric
Chemistry
and Physics
Discussions

Introduction

Halogen chemistry in the troposphere influences budgets of O_3, HO_x (OH and HO_2), NO_x (NO and NO_2) (von Glasow et al., 2004; Saiz-Lopez and von Glasow, 2012; Simpson et al., 2015, Schmidt et al., 2016; Sherwen et al., 2016a; Sherwen et al., 2016b), affects the oxidation state of atmospheric mercury (Holmes et al., 2006; Holmes et al., 2010), and impacts aerosol formation (Hoffmann et al., 2001; O'Dowd et al., 2002; McFiggans et al., 2004; McFiggans et al., 2010; Mahajan et al., 2011; Sherwen et al., 2016c).

The production of bromine and iodine atoms in the marine boundary layer (MBL) following emissions of organohalogen compounds and the inorganic compounds I_2 and HOI has been shown to result in considerable destruction of tropospheric ozone (Read et al., 2008), leading to the production of bromine monoxide (BrO) and iodine monoxide (IO) radicals. Observations of BrO and IO radicals within the MBL have demonstrated widespread impacts on atmospheric composition and chemistry (Alicke et al., 1999; Sander et al., 2003; Leser et al., 2003; Saiz-Lopez and Plane, 2004; Saiz-Lopez et al., 2004; Peters et al., 2005; Saiz-Lopez et al., 2006; Whalley et al., 2007; Mahajan et al., 2010a; Commane et al., 2011; Dix et al., 2013; Gomez Martin et al., 2013), including significant effects on HO_x concentrations and on the HO_2:OH ratio in coastal and marine locations (Bloss et al., 2005a; Sommariva et al., 2006; Bloss et al., 2007; Bloss et al., 2010; Kanaya et al., 2007; Whalley et al., 2010).

The role of halogens in in HO_x chemistry was demonstrated during the NAMBLEX campaign in Mace Head, Ireland, (Heard et al., 2006), following several studies which attributed box model overestimates of HO_2 observations in marine environments to unmeasured halogen monoxides (Carslaw et al., 1999; Carslaw et al., 2002; Kanaya et al., 2001; Kanaya et al., 2002; Kanaya et al., 2007). Simultaneous measurements of OH and HO_2 by laser-induced fluorescence (LIF) (Bloss et al., 2005a; Smith et al., 2006) and halogen species by a combination of DOAS (for BrO or IO, OIO and I_2) (Saiz-Lopez et al., 2006) and broadband cavity ringdown spectroscopy (BBCRDS) (for OIO and I_2) (Bitter et al., 2005) during NAMBLEX enabled box model calculations to fully explore the impacts of halogens on the local composition. A box model without halogen chemistry was able to reproduce the NAMBLEX OH observations to within 25 %, but HO_2 observations were overestimated by up to a factor of 2 (Sommariva et al., 2006). The introduction of halogen chemistry, using DOAS measurements of BrO and IO (Saiz-Lopez et al., 2006) to constrain the model, increased the modelled OH concentrations by up to 15 % and decreased HO_2 by up to 30 % owing to reactions of HO_2 with XO radicals to form HOX which subsequently photolysed to X + OH (Sommariva et al., 2006). Bloss et al., (2005a) indicated that up to 40 % of the instantaneous HO_2 loss could be attributed to HO_2 + IO, and that photolysis of HOI was responsible for 15 % of the noontime OH production.

Atmospheric
Chemistry
and Physics
Discussions

69   The impacts of halogen chemistry on HO_x radicals at a site representative of the open ocean have been investigated

70   at the Cape Verde Atmospheric Observatory (CVAO). Measurements of halogen monoxides (Mahajan et al.,

71   2010a) at the site have been shown to have significant impacts on local ozone concentrations, notably in the

72   magnitude of the daily cycle (Read et al., 2008), and have been used to constrain box model calculations used to

73   explore observations of OH and HO_2 made during the RHaMBLe campaign in 2007 (Whalley et al., 2010). The

74   model calculations showed generally good comparisons with the observed OH and HO_2 concentrations, apart

75   from a period characterised by unusually high concentrations of HCHO. Compared to a model run in which

76   halogen chemistry was absent, bromine and iodine chemistry led to a 9 % increase in the modelled OH

77   concentration (Whalley et al., 2010). Owing to the dominance of the tropics in global methane oxidation (Bloss

78   et al., 2005b), such an impact of halogens on OH could have significant consequences for estimates of global

79   methane lifetimes, and on our understanding of the impacts of halogen chemistry on climate change.

80

81   In general, observationally constrained box model simulations suggest that halogens in the troposphere chemistry

82   will increase OH concentrations, primarily because of a change in the HO_2 to OH ratio occurring as a result of

83   reactions of halogen oxides (XO) with HO_2 to produce a hypohalous acid (HOX) which photolyses to give an OH

84   radical and a halogen atom (Kanaya et al., 2002; Bloss et al., 2005a; Kanaya et al., 2007; Sommariva et al., 2006;

85   Sommariva et al., 2007; Whalley et al., 2010). Other impacts on the HO_x photochemical system are observed

86   (impacts from changes to NO_x chemistry etc.) but these are minor and overall the general conclusion is that the

87   halogen chemistry tends to increase the OH concentration and thus the oxidising capacity of the atmosphere.

88

89   However, the observationally constrained studies are typically concerned with processes occurring at the surface,

90   and in a single location. The role of halogen chemistry in the troposphere as a whole is more uncertain, particularly

91   in the free troposphere and on a global scale (Saiz-Lopez and von Glasow, 2012; Simpson et al., 2015). Inclusion

92   of bromine chemistry in the three-dimensional (3D) chemistry transport model (CTM) MATCH-HPIC resulted

93   in decreases in tropospheric ozone concentrations of ~18 % over widespread areas, with regional decreases of up

94   to 40 % (von Glasow et al., 2004). Increases of more than 20 % were found for OH in the free troposphere, but,

95   globally, changes to OH were dominated by decreases in OH in the tropics owing to a reduction in primary

96   production from O_3 photolysis, leading to a decrease of 1-2 % in the global mean OH concentration (von Glasow

97   et al., 2004).

98

99   Significant decreases in tropospheric ozone (up to 30% at high latitude spring) were also reported for the

100   pTOMCAT model on inclusion of bromine chemistry (Yang et al., 2005). The CAM-Chem global chemistry-

101   climate model has shown an approximate 10 % decrease in global mean tropospheric ozone concentration on

102   incorporation of lower bromine emissions (Saiz-Lopez et al., 2012), while the GEOS-Chem CTM displays a

103   global decrease of 6.5 % (Parrella et al., 2012). The GEOS-Chem model indicated that bromine-catalysed loss

104   of ozone is limited by the rate of production of HOBr, and that $HO_2 + BrO$ is responsible for over 95 % of the

105   global tropospheric HOBr production. While HOBr can act as a source of OH on photolysis, the changes to O_3

106   and NO_x resulting from the inclusion of bromine chemistry in GEOS-Chem led to a 4 % decrease overall in the

107   global annual mean OH (Parrella et al., 2012).

108

109   Vertically resolved airborne measurements of IO radicals in the free troposphere over the Pacific Ocean have also

110   demonstrated a role for iodine chemistry throughout the free troposphere, with IO observed at a mixing ratio of

111   ~0.1 ppt in the free troposphere and found to be present in both recent deep convective outflow and aged free

112   tropospheric air (Dix et al., 2013). Model simulations to investigate iodine-driven ozone destruction throughout

113   the troposphere indicated that only 34 % of the total iodine-driven ozone loss occurs within the marine boundary

114   layer, with 40 % occurring in a transition layer and 26 % in the free troposphere (Dix et al., 2013).

115

116   The CAM-Chem and GEOS-Chem models have also been updated to encompass iodine chemistry, with results

117   from CAM-Chem showing iodine chemistry to be responsible for 17-27 % of the ozone loss in the tropical MBL

118   and 11-27 % of the ozone loss in the marine upper troposphere (Saiz-Lopez et al., 2014). The GEOS-Chem model

119   also showed iodine chemistry to be responsible for significant ozone destruction throughout the troposphere

120   (Sherwen et al., 2016a; Sherwen et al., 2016b; Sherwen et al., 2017). The GEOS-Chem simulations, which

121   incorporate chlorine, bromine and iodine chemistry, show a reduction in global tropospheric ozone concentration

122   of 18.6 %, compared to simulations with no halogen chemistry, a reduction in the global mean OH of 8.2 % to a

123   concentration of 1.28×10^6 cm^{-3} and a resulting increase in global methane lifetime of 10.8 % to 8.28 years

124   (Sherwen et al., 2016b).

125

126   There is thus a discrepancy between box and global models as to the impact of halogen chemistry on OH

127   concentrations in the troposphere. Box models suggesting that OH radical concentrations should increase and

128   thus that halogens tend to increase the oxidising capacity, whereas the global models tend to suggest the opposite.

129

130   In this work, we use both a detailed chemical box model approach and a global chemistry-transport model to

131   investigate the local and global impacts of halogen chemistry on HO_x radical concentrations. We focus on

132   seasonal HO_x observations available from the Cape Verde Atmospheric Observatory (Vaughan et al., 2012). We

133   first provide a summary of the measurement site and the observations, followed by details of the two models used

Atmospheric
Chemistry
and Physics
Discussions

134   in this study. We then evaluate the impact of halogens on the concentrations of oxidants in the two modelling

135   frameworks and consider the impact of halogen chemistry on global oxidising capacity.

136

137   **The Cape Verde Atmospheric Observatory**

138   The Cape Verde Atmospheric Observatory is situated on the north east coast of the island of Sao Vicente (16.848

139   ºN, 24.871 ºW), approximately 500 km off the west coast of Africa. The observatory is in a region of high marine

140   biological production, and, for 95 % of the time, receives the prevailing northeasterly trade wind directly off the

141   ocean (Read et al., 2008; Carpenter et al., 2010). Measurements at the observatory are considered to be

142   representative of the open ocean, and CO, O_3, VOCs, NO_x and NO_y have been measured near-continuously at the

143   observatory since October 2006 (Lee et al., 2009; Carpenter et al., 2010).

144

145   In 2007, the observatory was host to the RHaMBLe intensive field campaign, during which a number of additional

146   measurements were made to complement the long-term measurements at the site (Lee et al., 2010), including LP-

147   DOAS measurements of halogen species (Read et al., 2008; Mahajan et al., 2010a) and formaldehyde (Mahajan

148   et al., 2010b), and LIF-FAGE measurements of OH and HO_2 (Whalley et al., 2010). The halogen monooxide

149   radicals BrO and IO exhibited a 'top-hat' diurnal cycle (Vogt et al., 1999; Vogt et al., 1996; Read et al., 2008;

150   Mahajan et al., 2010a) with essentially zero concentration in the hours of darkness and generally constant values

151   of approximately 2.5 ppt BrO and 1.4 ppt IO during the day.

152

153   The RHaMBLe campaign was followed by the Seasonal Oxidants Study (SOS) in 2009, during which

154   measurements of OH and HO_2 were conducted over three periods (Feb-March (SOS1), May-June (SOS2), and

155   September (SOS3)), and are discussed in detail by Vaughan et al. (2012). We present here the results from a

156   modelling study of the HO_x measurements made during SOS1 and SOS2, when supporting measurements are

157   available, using both box and global model approaches. SOS3 is not considered in this work owing to a lack of

158   supporting measurements.

159

160   Measurements of OH and HO_2 during the Seasonal Oxidant Study were made by laser-induced fluorescence (LIF)

161   spectroscopy at low pressure using the fluorescence assay by gas expansion (FAGE) technique, and are described

162   in detail by Vaughan et al. (2012). Briefly, ambient air is drawn into a fluorescence cell situated on the roof of a

163   shipping container and maintained at pressures of ~ 2 Torr. The fluorescence cell has two excitation axes, with

164   excess NO added at the second axis to titrate HO_2 to OH, enabling simultaneous detection of OH and HO_2. OH

165   radicals in both excitation axes are excited by laser light at λ ~ 308 nm, generated by frequency tripling the output

Atmospheric
Chemistry
and Physics
Discussions

166 of a solid state Nd:YAG pumped Ti:Sapphire laser system (Bloss et al., 2003). Channel photomultiplier tubes

167 coupled to gated photon counters are used to detect the $A^2\Sigma^+ - X^2\Pi_i$ OH fluorescence signal at $\lambda \sim 308$ nm.

168

169 Calibration of the instrument is achieved by measurement of the fluorescence signal from known concentrations

170 of OH and HO_2, produced by the photolysis of water vapour, and was performed over a range of conditions before,

171 during and after the campaign. For OH, the 1 σ limit of detection (LOD) was in the range $(2\text{-}11) \times 10^5$ cm^{-3} for a

172 5 min averaging period, while for HO_2 1 σ LOD was in the range $(6\text{-}13) \times 10^5$ cm^{-3} for a 4 min averaging period.

173 Uncertainties (2 σ) in the measurements of OH and HO_2 are $\sim$32 % (Vaughan et al., 2012).

174

175 Potential interferences in HO_2 measurements arising from conversion of alkene- and aromatic-derived peroxy

176 radicals to OH within the LIF detection cell, as described by Fuchs et al. (2011), are expected to be small for this

177 work owing to relatively low concentrations of alkenes and aromatics at the Cape Verde observatory (Carpenter

178 et al., 2010; Vaughan et al., 2012). Speciation of the peroxy radicals in the box model output (see Supplementary

179 Material) shows that 87.4 % of the peroxy radicals are HO_2 and CH_3O_2, 6.5 % $CH_3C(O)O_2$ and 1.1 % $C_2H_5O_2$,

180 all of which display no HO_2 interference in the laboratory (Whalley et al., 2013: Stone et al., 2014). Peroxy

181 radicals derived from OH-initiated oxidation of ethene and propene ($HOC_2H_4O_2$ and $HOC_3H_6O_2$, respectively)

182 were found to result in an interference signal for HO_2 in the laboratory ($\sim$40 % for the experimental configuration

183 in this work) but each radical comprises only $\sim$0.6 % of the total RO_2 in this work. Thus, model calculations

184 reported here do not include representation of potential HO_2 interferences, although such phenomena may be

185 important in other environments (see for example, Whalley et al., 2013; Stone et al., 2014).

186

187 **Model Approaches**

188 We interpret the observations using two different modeling frameworks. The first is an observationally

189 constrained box model (DSMACC), the second is a global tropospheric chemistry transport model (GEOS-

190 Chem).

191

192 **Constrained Box Model**

193 The Dynamically Simple Model of Atmospheric Chemical Complexity (DSMACC) is described in detail by

194 Emmerson and Evans (2009) and Stone et al. (2010), and is a zero-dimensional model using the Kinetic Pre-

195 Processor (KPP) (Sandu and Sander, 2006). In this work we use a chemistry scheme based on a subsection of the

196 hydrocarbons (ethane, propane, *iso*-butane, *n*-butane, *iso*-pentane, *n*-pentane, hexane, ethene, propene, 1-butene,

197 acetylene, isoprene, toluene, benzene, methanol, acetone, acetaldehyde and DMS) available from the Master

198 Chemical Mechanism version 3.2 (MCM v3.2 http://mcm.leeds.ac.uk/MCM/home.htt) (Jenkin et al., 2003;

Atmospheric
Chemistry
and Physics
Discussions
Open Access
EGU

199   Saunders et al., 2003), with a halogen chemistry scheme described by Saiz-Lopez et al. (2006), Whalley et al.

200   (2010) and Edwards et al. (2011). We also include the reaction between OH and CH_3O_2 (Bossolasco et al., 2014;

201   Fittschen et al., 2014; Assaf et al., 2016; Yan et al., 2016), with a rate coefficient of 1.6×10^{-10} cm^3 s^{-1} (Assaf et

202   al., 2016) and products $HO_2 + CH_3O$ (Assaf et al., 2017), the impact of which on the $HO_2:OH$ ratio and CH_3O_2

203   budget is described in the Supplementary Material. The total number of species in the model is ~1200, with ~5000

204   reactions. The full chemistry scheme used in the model is given in the Supplementary Data.

205

206   All measurements are merged onto a 10 minute timebase for input to the model and the model is run with

207   constraints applied as discussed in our previous work (Stone et al., 2010; Stone et al., 2011; Stone et al., 2014).

208   Concentrations of CH_4 and H_2 are kept constant at values of 1770 ppb (NOAA CMDL flask analysis,

209   ftp://ftp.cmdl.noaa.gov/ccg/ch4/) and 550 ppb (Ehhalt and Rohrer, 2009; Novelli et al., 1999) respectively.

210   Formaldehyde measurements were not available during the SOS and we thus use HCHO concentrations generated

211   by the chemistry in the model, with the modelled HCHO concentrations in broad agreement with previous

212   measurements at the observatory (Mahajan et al., 2010b). Table 1 shows a summary of the input parameters to

213   the model.

Atmospheric
Chemistry
and Physics
Discussions

Species	Mean	Median	Range
O_3 / ppb	33.8 ± 8.6	30.7	19.6 – 49.7
CO / ppb	102.3 ± 10.3	99.3	87.8 – 127.3
H_2O / ppm	20542.3 ± 2753.8	21290.0	16778.5 – 24909.2
NO / ppt	11.2 ± 10.6	9.0	0.06 – 96.2
Ethane / ppt	961.3 ± 289.4	864.0	625.4 – 1799.2
Propane / ppt	136.1 ± 87.05	111.8	20.2 – 521.5
iso-butane / ppt	13.4 ± 9.8	11.1	0 – 62.7
n-butane / ppt	21.9 ± 17.6	17.8	0 – 112.9
Actylene / ppt	79.0 ± 27.8	70.4	45.0 – 180.5
Isoprene / ppt	0.1 ± 0.4	0	0 – 2.6
iso-pentane / ppt	3.9 ± 3.2	3.3	0 – 22.9
n-pentane / ppt	4.3 ± 3.0	3.9	0 – 21.7
n-hexane / ppt	1.0 ± 0.7	0.9	0 – 4.4
Ethene / ppt	43.6 ± 15.2	46.3	6.4 – 73.2
Propene / ppt	13.5 ± 3.6	13.0	6.2 - 24.1
But-1-ene / ppt	6.5 ± 1.4	6.3	3.5 – 10.6
Benzene / ppt	13.0 ± 17.0	8.3	0 – 64.4
Toluene / ppt	77.9 ± 388.8	0	0 – 2013.9
Acetaldehyde / ppt	511.8 ± 526.0	599.3	0 – 2622.6
Methanol / ppt	247.6 ± 336.2	173.3	0 – 3337.4
DMS / ppt	8.3 ± 38.3	0	0 – 291.8

214   Table 1: Summary of inputs to the model. Zero values indicate measurements below the limit of detection.

215   Further details can be found in Vaughan et al. (2012) and Carpenter et al. (2010).

216

217

218

219

220

221

222

223

Atmospheric
Chemistry
and Physics
Discussions

224   Physical loss of each species in the model is represented by a first-order loss process, with the first-order rate

225   coefficient equivalent to a lifetime of approximately 24 hours, as discussed by Stone et al. (2010). Loss of reactive

226   species to aerosol surfaces is represented in the model by parameterisation of a first-order loss process to the

227   aerosol surface (Schwarz, 1986), as discussed by Stone et al. (2014).

228

229   A range of aerosol uptake coefficients for HO_2 have been reported in the literature, with recent measurements

230   indicating values of γ_{HO2} between 0.003 and 0.02 on aqueous aerosols (George et al., 2013) while others have

231   reported values of $\gamma_{HO2} \sim 0.1$ (Taketani et al., 2008), and increased uptake coefficients in the presence of Cu and

232   Fe ions (Thornton et al., 2008; Mao et al., 2013). In this work we use a value of $\gamma_{HO2} = 0.1$ in order to maintain

233   consistency with previous modelling studies at the site (Whalley et al., 2010) and to account for potential impacts

234   of ions of copper and iron in aerosol particles influenced by mineral dust (Carpenter et al., 2010; Muller et al.,

235   2010; Fomba et al., 2014; Matthews et al., 2014; Lakey et al., 2015).

236

237   The aerosol surface area in the model is constrained to previous measurements of dry aerosol surface area at the

238   observatory, corrected for differences in sampling height between the aerosol and HO_x measurements and for

239   aerosol growth under humid conditions (Allan et al., 2009; Muller et al., 2010; Whalley et al., 2010).

240

241   Halogen species are constrained to a 'top-hat' profiles for BrO and IO (Vogt et al., 1999; Vogt et al., 1996; Read

242   et al., 2008), as observed during the RHAMBLE campaign in 2007 (Read et al., 2008; Mahajan et al., 2010a).

243   The observations indicate that while there is day to day variation in BrO and IO concentrations, there is little

244   seasonal variation (Mahajan et al., 2010a). BrO and IO are thus constrained to the mean observed mixing ratios

245   of 2.5 ppt and 1.4 ppt, respectively, for time points between 0930 and 1830 (GMT) and zero for all other times.

246   In a similar way to NO_x (see Stone et al. (2010; 2011)), concentrations of all bromine or iodine species, including

247   BrO and IO, are permitted to vary according to the photochemistry as the model runs forwards. At the end of

248   each 24 hour period in the model, the calculated concentrations of BrO and IO are compared to the constrained

249   value, and the concentrations of all bromine (Br, Br_2, BrO, HBr, HOBr, $BrONO_2$, $BrNO_2$, BrNO) and iodine (I,

250   I_2, IO, HI, HOI, INO, INO_2, $IONO_2$, OIO, I_2O_2, I_2O_3, I_2O_4, $HOIO_2$) species are fractionally increased or decreased

251   such that the calculated and constrained concentrations of BrO and IO are the same. The model is run forwards

252   in time with diurnally varying photolysis rates until a diurnal steady state is reached, typically requiring between

253   5 and 10 days.

254

255

256

Global Model

258 We use the 3D global chemistry transport model GEOS-Chem (v10-01, www.geos-chem.org). The model has

259 been extensively evaluated against observations (Bey et al., 2001; Evans and Jacob, 2005; Nassar et al., 2009;

260 Mao et al., 2010; Zhang et al., 2010; Parrella et al., 2012; Hu et al., 2017). The model is driven by assimilated

261 winds calculated by the Goddard Earth Observing System at a horizontal resolution of $4° \times 5°$, with 47 vertical

262 levels from the surface to 50 hPa. Anthropogenic emissions of CO, NO_x and SO_2 are described by the EDGAR

263 3.2 monthly global inventory (Olivier et al., 2005). Emissions of volatile organic compounds (VOCs) are

264 described by the RETRO monthly global inventory (van het Bolscher, 2008) for anthropogenic sources, with

265 ethane emissions described by Xiao et al., 2008, and the MEGAN v2.1 inventory (Guenther et al., 2006; Barkley

266 et al., 2011) for biogenic sources.

267

268 The HO_x-NO_x-VOC-O_3 chemistry scheme in the model is described in detail by Bey et al. (2001) and Mao et al.

269 (2013), with the isoprene oxidation mechanism described by Paulot et al. (2009). Photolysis rates use the FAST-

270 JX scheme (Bian and Prather, 2002; Mao et al., 2010), with acetone photolysis rates updated by Fischer et al.

271 (2012). Stratospheric chemistry is based on LINOZ McLinden et al. (2000) for O_3 and a linearised mechanism

272 for other species as described by Murray et al. (2012).

273

274 The model framework includes gas-aerosol partitioning of semi-volatile organic compounds (Liao et al., 2007;

275 Henze et al., 2007; Henze et al., 2009; Fu et al., 2008; Heald et al., 2011; Wang et al., 2011), and heterogeneous

276 chemistry (Jacob, 2000). Coupling between gas phase chemistry and sulfate-ammonium-nitrate aerosol is

277 described by Park et al. (2004) and Pye et al. (2009). A description of dust aerosol in the model is given by Fairlie

278 et al. (2007). Treatment of sea salt aerosol is described by Jaegle et al. (2011). The uptake coefficient for N_2O_5

279 uses the parameterisation by Evans and Jacob (2005), while that for HO_2 uses the parameterisation of Thornton

280 et al. (2008). A full description of the organic aerosol chemistry in the model is given by Heald et al. (2011).

281

282 The model includes recent updates to the chemistry scheme to include bromine chemistry (Parella et al., 2012;

283 Schmidt et al., 2016) and iodine chemistry (Sherwen et al., 2016a; Sherwen et al., 2016b). Sources of tropospheric

284 bromine in the model include emissions of $CHBr_3$, CH_2Br_2 and CH_3Br, and transport of reactive bromine from

285 the stratosphere. Debromination of sea-salt aerosol is not included in the model following the work of Schmidt et

286 al. (2016), which showed better agreement with observations of BrO made by the GOME-2 satellite (Theys et al.,

287 2011) and in the free troposphere and the tropical Eastern Pacific MBL (Gomez Martin et al., 2013; Volkamer et

288 al., 2015; Wang et al., 2015). Emission rates and bromine chemistry included in the model are described in detail

289 by Parella et al. (2012), with the additional bromine chemistry scheme described by 19 bimolecular reactions, 2

Atmospheric
Chemistry
and Physics
Discussions

290   three-body reactions and 2 heterogeneous reactions using rate coefficients, heterogeneous reaction coefficients

291   and photolysis cross-sections recommended by Sander et al. (2011).

292

293   Iodine sources include emissions of CH_3I, CH_2I_2, CH_2ICl, CH_2IBr, I_2 and HOI. Emissions for CH_3I follow Bell

294   et al. (2002), while those of other organic iodine species use parameterisations based on chlorophyll-a in the

295   Tropics and constant oceanic and coastal fluxes in extratropical regions (Ordonez et al., 2012). Emissions of

296   inorganic iodine species (HOI and I_2) use the results of Carpenter et al. (2013), with oceanic iodide concentrations

297   parameterised by MacDonald et al. (2014). The iodine chemistry scheme includes 26 unimolecular and

298   bimolecular reactions, 3 three-body reactions, 21 photolysis reactions and 7 heterogeneous reactions, using

299   recommendations by Atkinson et al. (2007) and Sander et al. (2011) where available. Full details are given by

300   Sherwen et al. (2016a; 2016b).

301

302   Photolysis rates of bromine and iodine compounds are calculated using the FAST-J radiative transfer model (Wild

303   et al., 2000; Bian and Prather, 2002; Mao et al., 2010). Wet and dry deposition are determined as for the standard

304   GEOS-Chem model (Liu et al., 2001; Wesely, 1989; Wang et al., 1998; Amos et al., 2012).

305

306   The tropospheric chemistry scheme is integrated using the SMVGEAR solver (Jacobson and Turco, 1994; Bey et

307   al., 2001). The model, provides hourly output at the site of the Cape Verde Atmospheric Observatory. Model

308   simulations have been performed in the absence of halogens, with bromine chemistry, with iodine chemistry and

309   with bromine and iodine chemistry combined. Each model simulation is run for two years, with the analysis

310   performed on the second year (2009) and the first year discarded as model spin-up to enable evolution of long-

311   lived species.

312

313   **Model Results**

314   We now investigate the impact of halogen chemistry on tropospheric oxidation at Cape Verde within our two

315   modelling approaches.

316

317   **Constrained Box Model**

318   Figure 1 shows the observed and modelled time series for OH and HO_2 during SOS1 (February, March 2009) and

319   SOS2 (May, June 2009). Observed concentrations of OH and HO_2 were typically higher in SOS2 than SOS1,

320   reaching maximum values in SOS2 of ~ 9×10^6 cm^{-3} OH and 4×10^8 cm^{-3} HO_2 (Vaughan et al., 2012). Similar

321   concentrations were observed in May and June 2007 during the RHaMBLe campaign (Whalley et al., 2010), with

322   a *t*-test indicating no statistically significant difference between the OH concentrations measured in May-June

11

323 2009 to those measured in May-June 2007 at the 95 % confidence level (Vaughan et al., 2012). Concentrations

324 of HO_2 measured in May-June 2009 were significantly higher than those measured in May-June 2007 at the 95

325 % confidence level, but were within the 1σ day-to-day variability (Vaughan et al., 2012). Temperatures during

326 SOS2 were typically higher than those during SOS1, with higher relative humidity during SOS2 (Vaughan et al.,

327 2012). Air masses during SOS1 had strong contributions from Atlantic marine air and African coastal region,

328 with polluted marine air and Saharan dust contributing ~ 20 % and 10 %, respectively, for the first half of the

329 measurement period. Conditions during SOS2 were typically cleaner, with Atlantic marine air representing the

330 major source, although coastal African air contributed ~ 40 % on some days. There was little influence from

331 polluted air, dust or continental air (Vaughan et al., 2012). Analysis of the variance of OH and HO_2 during SOS

332 indicated that ~70 % of the total variance could be explained by diurnal behaviour, with the remaining ~30 %

333 related to changes in air mass.

334

335 Figure 1 shows the observed and modelled time series for OH and HO_2, for model simulations with and without

336 halogen chemistry. For SOS1, the box model overpredicts the OH and HO_2 concentrations at the start of the

337 campaign (Julian days 59 and 61), but performs better for day 63, and captures both the observed diurnal profile

338 and the observed concentrations. For SOS2, the box model tends to agree better with the observations for both

339 OH and HO_2. A day-by-day comparison between the models and the observations is shown in the Supplementary

340 Material for days for which box model calculations were possible, which were limited by the availability of

341 supporting data.

342

343 Figure 2 shows the point-by-point model performance for OH and HO_2 for all data points combined, and for

344 SOS1 and SOS2 separately, for the full box model run including halogen chemistry. There is a tendency for

345 overprediction of OH and HO_2 during SOS1 (slopes of modelled vs observed concentrations are (1.86 ± 0.26) for

346 OH and (1.66 ± 0.21) for HO_2), which is dominated by the model overpredictions on days 59 and 61, with better

347 agreement observed during SOS2 (slopes of modelled vs observed concentrations are (1.11 ± 0.15) for OH and

348 (1.21 ± 0.12) for HO_2).

349

350 The measured and modelled average diurnal profiles of OH, HO_2 and the HO_2 to OH ratios are shown in Figure

351 3. At midday (1100-1300), the full model including halogen chemistry overpredicts OH by a median factor of

352 1.52 and HO_2 by a median factor of 1.21. A model run containing bromine chemistry but no iodine chemistry

353 gave median midday overpredictions of 1.40 and 1.30 for OH and HO_2, respectively, while a run containing

354 iodine but not bromine gave equivalent median overpredictions of 1.50 and 1.26, respectively. With no halogen

355 chemistry included in the model, the modelled OH decreases, giving a median overprediction at midday by a

Atmospheric
Chemistry
and Physics
Discussions

356 factor of 1.37, while the modelled HO_2 increases, resulting in a median overprediction by a factor of 1.37 at

357 midday.

358

359 Thus the inclusion of halogens (bromine and iodine) in the box model changes the mean noon time OH and HO_2

360 concentrations by +9.8 % and –9.9 %, respectively. This impact of halogen chemistry is consistent in sign and

361 magnitude with previous studies (Kanaya et al., 2002; Bloss et al., 2005a; Kanaya et al., 2007; Sommariva et al.,

362 2006; Sommariva et al., 2007; Whalley et al., 2010).

363

364 Figure 4 shows the mean midday total RO_x budget (given the fast processing time between HO_2 and HOBr/HOI

365 we identify the RO_x family as OH, HO_2, HOBr, HOI, RO and RO_2) for the two measurement periods during SOS

366 for model runs with and without halogens. These budgets are similar both between time periods (i.e. SOS1 vs

367 SOS2) and for box model calculations with and without halogen chemistry. Radical production dominated by

368 photolysis of ozone (~83 %), with photolysis of HCHO (~10 %), CH_3CHO (~2 %) and H_2O_2 (~2 %) playing a

369 significantly smaller role. Radical termination reactions were dominated by $HO_2 + CH_3O_2$ (~23 %), aerosol uptake

370 of HO_2 (~21 %), $HO_2 + HO_2$ (~19 %), $CH_3C(O)O_2 + HO_2$ (~8 %), and $OH + HO_2$ (~5 %). The inclusion of the

371 reaction between OH and CH_3O_2 reduces the importance of radical termination via $HO_2 + CH_3O_2$ (from ~26 %

372 of the total to ~23 % of the total), but otherwise has little impact on the total radical removal owing to the expected

373 production of $HO_2 + CH_3O$ (Assaf et al., 2017). Further details regarding the impact of the reaction between OH

374 and CH_3O_2 on the HO_2:OH ratio and CH_3O_2 budget are given in the Supplementary Material.

375

376 The budget analyses for SOS are consistent with those determined for the RHaMBLe campaign (Whalley et al.,

377 2010; Fittschen et al., 2014; Assaf et al., 2017), reflecting similarities in observed concentrations of long-lived

378 species and the method of the model constraint with observed O_3 concentrations and photolysis rates. The primary

379 source of radicals therefore remains fixed in all simulations, with the primary sinks for these species occurring

380 through radical-radical reactions. Thus, the total radical concentration and budget is little impacted by the

381 presence of halogens.

382

383 However, the partitioning of the radicals is impacted by the halogens. Without halogens the average midday

384 (1100-1300) HO_2 to OH ratio is (83.4 ± 15.4) (median = 82.7), with the halogens this changes to (68.3 ± 13.6)

385 (median = 66.9) (Table 2). This change in partitioning is mainly due to the reaction of HO_2 with BrO and IO

386 followed by the photolysis of HOBr and HOI to give OH. In this way the halogens tend to reduce the concentration

387 of HO_2 and increase the concentration of OH.

388

Atmospheric
Chemistry
and Physics
Discussions

	HO$_2$:OH ratio
Observed	79.1 ± 34.1 (70.7)
Box model, no halogens	83.4 ± 15.4 (82.7)
Box model with Br chemistry	78.9 ± 15.6 (77.8)
Box model with I chemistry	71.5 ± 13.0 (70.4)
Box model with Br and I chemistry	68.3 ± 13.6 (66.9)
Global model, no halogens	80.8 ± 18.1 (78.9)
Global model with Br chemistry	81.9 ± 19.0 (79.7)
Global model with I chemistry	70.4 ± 12.5 (70.5)
Global model with Br and I chemistry	71.3 ± 13.2 (71.3)

389

390 Table 2: Mean (± 1σ) midday (1100-1300 hours) ratios of HO$_2$ to OH (SOS1 and SOS2 combined). Median

391 values are given in parentheses.

392

393 In the box model without halogen chemistry, production of OH is dominated by ozone photolysis (76 %), HO$_2$ +

394 NO (12 %) and HO$_2$ + O$_3$ (9 %), with OH loss controlled by OH + CO (37 %), OH + CH$_4$ (16 %) and OH +

395 CH$_3$CHO (15 %), as shown in Figure 5. Production of HO$_2$ in the model excluding halogens is controlled by OH

396 + CO (45 %), CH$_3$O + O$_2$ (19 %) and photolysis of HCHO (10 %), with loss governed by aerosol uptake (26 %),

397 HO$_2$ + HO$_2$ (26 %), HO$_2$ + NO (15 %), HO$_2$ + CH$_3$O$_2$ (12 %) and HO$_2$ + O$_3$ (10 %). In the presence of halogens,

398 the instantaneous budgets for OH and HO$_2$ are impacted by BrO and IO, as shown in Figures 5 and 6. For the

399 model run including halogens, OH production is still dominated by ozone photolysis (68 %), but there are

400 significant contributions from photolysis of HOI (10 %) and HOBr (3 %). Loss of HO$_2$ is also affected by the

401 presence of the halogen species, with the dominant loss processes including aerosol uptake (20 %), HO$_2$ + HO$_2$

402 (19 %), HO$_2$ + IO (14 %), HO$_2$ + NO (12 %), HO$_2$ + CH$_3$O$_2$ (11 %), HO$_2$ + O$_3$ (8 %) and HO$_2$ + BrO (6 %). As

403 shown in Figures 4-6 there is little difference in the radical budgets between SOS1 and SOS2.

404

405 This box modelling study is consistent with previous studies (Kanaya et al., 2002; Bloss et al., 2005a; Kanaya et

406 al., 2007; Sommariva et al., 2007; Whalley et al., 2010; Mahajan et al., 2010a; Stone et al., 2012) in that it implies

407 that halogen chemistry is likely to increase the OH concentration of the marine boundary layer (and potentially

408 other regions of the troposphere) as it enhances the HO$_2$ to OH conversion through the production of HOBr and

409 HOI. We now look at the impact of halogen chemistry on the concentrations of OH and HO$_2$ at Cape Verde within

410 the framework of a global atmospheric chemistry model.

411

412

Atmospheric
Chemistry
and Physics
Discussions

Global Model

413

414 Figure 1 shows the time series for OH and HO_2 calculated by the global model GEOS-Chem, with the average

415 diurnal profiles shown in Figure 3. The global model displays a significant overprediction for OH and HO_2 during

416 SOS1, but exhibits reasonable skill at reproducing the observed concentrations during SOS2 and captures the

417 HO_2:OH ratio for both measurement periods. The overpredictions of OH and HO_2 in the global model likely result

418 from a combination of missing OH-sinks, particularly oxygenated volatile organic compounds (oVOCs) which

419 are currently underestimated in the global model (Millet et al., 2015), and potential overprediction of the primary

420 radical production rate owing to reductions in photolysis rates resulting from cloud cover that are not captured by

421 the global model.

422

423 At midday (1100-1300), the modelled to observed ratios for OH and HO_2 for the global model excluding halogen

424 chemistry are (1.52 ± 1.02) and (1.72 ± 0.80), respectively, with a mean modelled HO_2 to OH ratio of $(80.8 \pm$

425 $18.1)$ (compared to the observed HO_2 to OH ratio of (79.1 ± 34.1)). For the global model run including bromine

426 chemistry, but not iodine, the mean midday modelled to observed ratios for OH and HO_2 are (1.48 ± 1.05) and

427 (1.69 ± 0.81), respectively, with a mean midday modelled HO_2 to OH ratio of (81.9 ± 19.0). Bromine chemistry

428 thus acts to decrease the concentrations of both OH and HO_2, in contrast to the box model results which show

429 increased concentrations of OH and decreased concentrations of HO_2. For the model run including iodine, but not

430 bromine, the midday modelled to observed ratios for OH and HO_2 are (1.57 ± 1.00) and (1.59 ± 0.81), respectively,

431 with a mean midday modelled HO_2 to OH ratio of (70.4 ± 12.5). Iodine chemistry thus results in increased OH

432 and decreased HO_2 for both the global and box model simulations at Cape Verde. Inclusion of bromine and iodine

433 chemistry combined leads to midday modelled to observed ratios of (1.53 ± 1.01) for OH and (1.57 ± 0.82) for

434 HO_2, and a mean midday modelled HO_2 to OH ratio of (71.3 ± 13.2). These results are shown in Table 2, alongside

435 those for the box model.

436

437 The results from the global model at Cape Verde thus differ from those of the box model. For the box model,

438 inclusion of bromine and iodine chemistry, whether separately or combined, leads to increased OH and decreased

439 HO_2 through increased conversion of HO_2 to OH through the production and subsequent photolysis of HOBr and

440 HOI. In the global model a more complex pattern emerges. In a similar way to the box model, the HO_2

441 concentrations in the global model are decreased on inclusion of bromine and/or iodine owing to the additional

442 loss reactions $HO_2 + BrO$ and $HO_2 + IO$. When bromine chemistry is considered in the global model in isolation

443 from iodine chemistry, the OH concentration decreases, despite the production and photolysis of HOBr. This

444 decrease occurs as a result of a reduction in the O_3 concentration in the model on inclusion of bromine chemistry

445 owing to the reaction of Br with O_3, which leads to a decrease in the rate of primary radical production from O_3

446 photolysis and thus lower OH concentrations. The impact of the decreased radical production rate is greater than

447 that leading to increased OH production through HOBr photolysis, and the net OH concentration is reduced in

448 the global model. This effect is not observed in the box model calculations as the model runs are constrained to

449 long-lived species – including O_3. The change in O_3 concentration on the inclusion of halogen chemistry is thus

450 not considered in the box model simulations, and the subsequent impacts of halogens consider only those changes

451 occurring on a more rapid timescale, which lead to increases in the OH concentration.

452

453 However, the inclusion of iodine chemistry in the global model does lead to increased OH concentrations at Cape

454 Verde. Direct emissions of HOI in the global model, in addition to chemical production through $HO_2 + IO$, result

455 in increased OH production through HOI photolysis as well as the repartitioning of HO_2 and OH through HOI

456 production in a similar manner to that for HOBr. However, the more rapid cycling of HO_2 to OH through the

457 more rapid production and photolysis of HOI compared to HOBr, reduces the impact of iodine chemistry on the

458 HO_2:OH ratio compared to that for bromine chemistry. Iodine chemistry thus can reduce the OH concentration

459 similarly to bromine chemistry, through the destruction of O_3 and subsequent reduction in primary production

460 rate, but the impact is less than that for bromine, and can be offset by the direct emissions of HOI which increases

461 the production rate of OH through photolysis.

462

463 The impacts of iodine chemistry in the global model are thus more complex than those for bromine chemistry.

464 When bromine and iodine chemistry are combined in the global model there is a competition between the effects

465 of the reduction in primary production of OH, through depletion of O_3, and the production of OH from photolysis

466 of HOBr and HOI and, for the model simulations at Cape Verde, the impacts of direct HOI emissions dominate.

467 The OH concentration is thus marginally increased compared to simulations containing no halogens, although the

468 HO_2 concentrations are significantly decreased.

469

470 The impacts of halogens on OH radical concentrations in the global model thus display a complexity that is

471 somewhat obscured in the box model simulations. Overall, the inclusion of halogens in the global model leads to

472 a slight increase in OH at Cape Verde, but, owing to the opposing effects of bromine and iodine, this result is

473 subject to the modelled concentrations of bromine and iodine species. Observations at Cape Verde made between

474 November 2006 and June 2007 indicate 'top-hat' profiles for BrO and IO, with average daytime mixing ratios of

475 2.5 ppt and 1.4 ppt, respectively, and little variability over the entire campaign (Read et al., 2008; Mahajan et al.,

476 2010a). The global model simulations reported here predict average mixing ratios of ~0.5 ppt for BrO and ~1 ppt

477 for IO during SOS, and thus underpredict BrO but perform well for IO. The underprediction of BrO at Cape Verde

478 results from recent model updates which exclude emissions of bromine species from sea-salt debromination

16

Atmospheric
Chemistry
and Physics
Discussions

479 (Schmidt et al., 2016) in order to provide improved agreement with observations of BrO made by the GOME-2

480 satellite (Theys et al., 2011) and in the free troposphere and the tropical Eastern Pacific MBL (Gomez Martin et

481 al., 2013; Volkamer et al., 2015; Wang et al., 2015). We now discuss the global impacts of halogen chemistry.

482

Global impacts of halogen chemistry on OH and HO$_2$

484 On the global scale, concentrations of OH and HO$_2$ are reduced on inclusion of bromine and iodine chemistry,

485 both individually and combined. The global mass weighted annual mean OH concentration decreases by 3.8 %

486 on inclusion of bromine chemistry, but only 0.02 % on inclusion of iodine chemistry alone. When the chemistry

487 of bromine and iodine is combined in the model, the global mass weighted annual mean OH concentration

488 decreases by 4.5 %. For HO$_2$, the global mass weighted annual mean is decreased by 4.2 % by bromine, 5.6 % by

489 iodine and 9.7 % by bromine and iodine combined. Figure 7 shows the probability distribution functions for the

490 changes to OH and HO$_2$ concentrations for the monthly mean values for all grid boxes within the troposphere for

491 the year. For the majority of grid boxes, concentrations of OH and HO$_2$ are reduced on inclusion of bromine

492 chemistry, with iodine also generally reducing HO$_2$ concentrations but leading to a wider spread of changes to

493 the OH concentration, and similar numbers of grid boxes showing increased and decreased concentrations. When

494 bromine and iodine chemistry are combined in the model, HO$_2$ shows a more significant decrease than for either

495 halogen individually, and OH, although exhibiting increased concentrations in a significant number of grid boxes,

496 displays a greater tendency for decreased concentrations.

497

498 Figure 8 shows the changes to the annual modelled surface layer OH and HO$_2$ concentrations on inclusion of

499 halogen chemistry, with annual surface layer mixing ratios of BrO and IO shown in Figure 9. The most significant

500 changes to OH and HO$_2$ occur over marine regions, particularly over the Southern Pacific. Smaller changes are

501 observed over land, and any increased concentrations, including those for OH over Cape Verde, can be seen to

502 occur in coastal regions where the impacts of direct HOI emissions dominate and concentrations of IO

503 concentrations are typically elevated.

504

505 Thus, overall, halogens act to reduce the oxidising capacity of the troposphere through reductions to O$_3$ and

506 subsequent reductions in the primary production rates of OH and HO$_2$, despite the slight increase in OH

507 concentration predicted by the global model at Cape Verde. Consideration of the full extent of the impacts of

508 halogens on the global oxidising capacity is hindered by uncertainties in the concentrations and distributions of

509 halogen species, and model representations of halogen processes, particularly those relating to sea salt

510 debromination, ocean iodide emissions, parameterisations of iodine recycling in aerosols and photolysis of higher

511 iodine oxides (Sherwen et al., 2016a).

Atmospheric
Chemistry
and Physics
Discussions

Conclusions

Measurements of OH and HO_2 made by LIF-FAGE at the Cape Verde Atmospheric Observatory during the Seasonal Oxidants Study in 2009 have been simulated by a constrained box model and a three-dimensional global chemistry transport model. The observations are generally reproduced well by the box model, but are overpredicted by the global model.

The oxidising capacity of the two models, as manifested by the OH concentration, shows opposing sensitivity to halogens. The constrained box model shows an increase in OH concentrations with the inclusion of halogens, whereas the global transport model shows a decrease in OH concentrations globally, despite a marginal decrease in the OH concentration at Cape Verde. This difference between models reflects differing representation of chemical timescales by the models. The box model is constrained to concentrations of long-lived compounds, including O_3, and considers only impacts on short timescales, whereas the global model includes impacts occurring on longer timescales. Within this context, the box model includes the short timescale impact of halogens on the repartitioning of HO_2 to OH, thus increasing OH and decreasing HO_2, but does not consider the longer timescale impact of halogen-mediated ozone destruction which impacts primary radical production. This highlights a general problem with understanding the complex interactions within atmospheric chemistry and the Earth system in general. Evaluating the impact of a small part of the system on the system as a whole can be difficult and the most significant processes may occur on timescales significantly longer than those of the perturbation.

Acknowledgements

References

Alicke, B., Hebestriet, H., Stutz, J., Platt, U.: Iodine oxide in the marine boundary layer, Nature, 397, 572-573, 1999

Allan, J.D., Topping, D.O., Good, N., Irwin, M., Flynn, M.,Williams, P.I., Coe, H., Baker, A.R., Martino, M., Niedermeier, N., Wiedensohler, A., Lehmann, S., Muller, K., Herrmann, H.,and McFiggans, G.: Composition and properties of atmospheric particles in the eastern Atlantic and impacts on gas phase uptake rates, Atmos. Chem. Phys., 9, 9299–9314, 2009

Atmospheric
Chemistry
and Physics
Discussions

546

547 Amos, H.M., Jacob, D.J., Holmes, C.D., Fisher, J.A., Wang, Q., Yantosca, R.M., Corbitt, E.S., Galarneau, E.,
548 Rutter, A.P., Gustin, M.S., Steffen, A., Schauer, J.J., Graydon, J.A., St. Louis, V.L., Talbot, R.W., Edgerton, E.S.,
549 Zhang, Y., and Sunderland, E.M: Gas-particle partitioning of Hg(II) and its effect on global mercury deposition,
550 Atmos. Chem. Phys., 12, 1, 591-603, doi:10.5194/acp-12-591-2012, 2012

551

552 Assaf, E., Song, B., Tomas, A., Schoemaker, C., and Fittschen, C.: Rate constant of the reaction between CH_3O_2
553 and OH radicals revisited, J. Phys. Chem. A, 120, 8923-8932, 2016

554

555 Assaf, E., Sheps, L., Whalley, L., Heard, D., Tomas, A., Schoemaecker, C., and Fittschen, C.: The reaction
556 between CH_3O_2 and OH radicals: Product yields and atmospheric implications, Environ. Sci. Technol., 51, 4,
557 2170-2177, doi: 10.1021/acs.est.6b06265, 2017

558

559 Atkinson, R., Baulch, D.L., Cox, R.A., Crowley, J.N., Hampson, R.F., Hynes, R.G., Jenkin, M.E., Rossi, M. J.,
560 and Troe, J.: Evaluated kinetic and photochemical data for atmospheric chemistry: Volume III – gas phase
561 reactions of inorganic halogens, Atmos. Chem. Phys., 7, 981–1191, doi:10.5194/acp-7-981-2007, 2007

562

563 Barkley, M.P., Palmer, P.I., Ganzeveld, L., Arneth, A., Hagberg, D., Karl, T., Guenther, A., Paulot, F., Wennberg,
564 P.O., Mao, J.Q., Kurosu, T.P., Chance, K., Muller, J.-F., De Smedt, I., van Roozendael, M., Chen, D., Wang,
565 Y.X., and Yantosca, R.M.: Can a "state of the art" chemistry transport model simulate Amazonian tropospheric
566 chemistry? J. Geophys. Res. Atmos., 116, D16302, 1-28, doi:10.1029/2011JD015893, 2011

567

568 Bell, N., Hsu, L., Jacob, D.J., Schultz, M.G., Blake, D.R., Butler, J.H., King, D.B., Lobert, J.M., and Maier-
569 Reimer, E.: Methyl iodide: Atmospheric budget and use as a tracer of marine convection in global models, J.
570 Geophys. Res. Atmos., 107, ACH 8-1–ACH 8-12, doi:10.1029/2001jd001151, 2002

571

572 Bey, I., Jacob, D.J., Yantosca, R.M., Logan, J.A., Field, B.D., Fiore, A.M., Li, Q., Liu, H.Y., Mickley, L.J.,
573 Schultz, M.G.: Global modelling of tropospheric chemistry with assimilated meteorology: Model description and
574 evaluation, J. Geophys. Res., 106, D19, 23073-23095, 2001

575

576 Bian, H.S., and Prather, M.J.: Fast-J2: Accurate simulation of stratospheric photolysis in global chemistry models,
577 J. Atmos. Chem., 41, 3, 281-296, 2002

578

579 Bitter, M., Ball, S., Povey, I., and Jones, R.: A broadband cavity ringdown spectrometer for in-situ measurements
580 of atmospheric trace gases, Atmos. Chem. Phys., 5, 3491–3532, doi:10.5194/acp-8-3491-2005, 2005

581

582 Bloss, W.J., Lee, J.D., Johnson, G.P., Sommariva, R., Heard, D.E., Saiz-Lopez, A., Plane, J.M.C., McFiggans,
583 G., Coe, H., Flynn, M., Williams, P., Rickard, A.R., Fleming, Z.: Impact of halogen monoxide chemistry upon
584 boundary layer OH and HO_2 concentrations at a coastal site, Geophys. Res. Lett., 32, L06814,
585 doi:10.1029/2004GL022084, 2005a

586

Atmospheric
Chemistry
and Physics
Discussions

587   Bloss, W.J., Evans, M.J., Lee, J.D., Sommariva, R., Heard, D.E., Pilling, M.J.: The oxidative capacity of the
588   troposphere: Coupling of field measurements of OH and a global chemistry transport model, Faraday. Discuss.,
589   130, 425-436, 2005b

591   Bloss, W.J., Lee, J.D., Heard, D.E., Salmon, Bauguitte, S.J.-B., Roscoe, H.K., Jones, A.E.: Observations of OH
592   and HO_2 radicals in coastal Antarctica, Atmos. Chem. Phys., 7, 4171-4185, 2007

594   Bloss, W.J., Camredon, M., Lee, J.D., Heard, D.E., Plane, J.M.C., Saiz-Lopez, A., Bauguitte, S.J.-B., Salmon,
595   R.A., Jones, A.E.: Coupling of HO_x, NO_x and halogen chemistry in the Antarctic boundary layer, Atmos. Chem.
596   Phys., 10, 10187-10290, 2010

598   Bossolasco, A., Farago, E.P., Schoemaker, C., and Fittschen, C.: Rate constant of the reaction between CH_3O_2
599   and OH radicals, Chem. Phys. Lett., 593, 7-13, 2014

601   Carpenter, L. J., Fleming, Z. L., Read, K. A., Lee, J. D., Moller, S.J., Hopkins, J., Purvis, R., Lewis, A. C., Muller,
602   K., Heinold, B., Herrmann, H., Wadinga Fomba, K., van Pinxteren, D., Muller, C., Tegen, I., Wiedensohler, A.,
603   Muller, T., Niedermeier, N., Achterberg, E. P., Patey, M. D., Kozlova, E. A., Heimann, M., Heard, D. E., Plane,
604   J. M. C., Mahajan, A., Oetjen, H., Ingham, T., Stone, D., Whalley, L., Evans, M., Pilling, M. J., Leigh, R. J.,
605   Monks, P. S., Karunaharan, A., Vaughan, S., Tschritter, J., Pohler, D., Frieß, U., Holla, R., Mendes, L., Lopez,
606   H., Faria, B., Manning, A. J., and Wallace, D. W. R.: Seasonal characteristics of tropical marine boundary layer
607   air measured at the Cape Verde Atmospheric Observatory, J. Atmos. Chem., 67, 87–140, 2010

609   Carpenter, L.J., MacDonald, S.M., Shaw, M.D., Kumar, R., Saunders, R.W., Parthipan, R., Wilson, J., and Plane,
610   J.M.C.: Atmospheric iodine levels influenced by sea surface emissions of inorganic iodine, Nat. Geosci., 6, 108–
611   111, doi:10.1038/ngeo1687, 2013

613   Carslaw, N., Creasey, D. J., Heard, D. E., Lewis, A .C., McQuaid, J. B., Pilling,M. J.,Monks, P. S., Bandy, B. J.,
614   and Penkett, S. A.: Modeling OH, HO_2, and RO_2 radicals in the marine boundary layer – 1. Model construction
615   and comparison with field measurements, J. Geophys. Res., 104(D23), 30 241–30 255, 1999

617   Carslaw, N., Creasey, D. J., Heard, D. E., Jacobs, P. J., Lee, J. D., Lewis, A. C., McQuaid, J. B., Pilling, M. J.,
618   Bauguitte, S., Penkett, S. A., Monks, P. S., Salisbury, G.: Eastern Atlantic Spring Experiment 1997 (EASE97) –
619   2. Comparisons of model concentrations of OH, HO_2, and RO_2 with measurements, J. Geophys. Res.-Atmos.,
620   107(D14), 4190, 2002

622   Commane, R., Seitz, K., Bale, C.S.E., Bloss, W.J., Buxmann, J., Ingham, T., Platt, U., Pohler, D., Heard, D.E.:
623   Iodine monoxide at a clean marine coastal site: observations of high frequency variations and inhomogeneous
624   distributions, Atmos. Chem. Phys., 11, 6721-6733, 2011

626   Dix, B., Baidar, S., Bresch, J.F., Hall, S.R., Schmidt, S., Wang, S., Volkamer, R.: Detection of iodine monoxide
627   in the tropical free troposphere, Proc. Nat. Acad. Sci., 110, 6, 2035-2040

629   Edwards, P., Evans, M.J., Commane, R., Ingham, T., Stone, D., Mahajan, A.S., Oetjen, H., Dorsey, J.R., Hopkins,
630   J.R., Lee, J.D., Moller, S.J., Leigh, R., Plane, J.M.C., Carpenter, L.J., Heard, D.E.: Hydrogen oxide
631   photochemistry in the northern Canadian spring time boundary layer, J. Geophys. Res., 116, D22306.
632   Doi:10.1029/2011JD016390, 2011
633
634   Ehhalt, D.H., Rohrer, F.: The tropospheric cycle of H_2: a critical review, Tellus, 61B, 500-535, 2009
635
636   Emmerson, K.M., Evans, M.J.: Comparison of tropospheric gas-phase chemistry schemes for use within global
637   models, Atmos. Chem. Phys., 9, 1831-1845, 2009
638
639   Evans, M. J., Jacob, D. J.: Impact of new laboratory studies of N2O5 hydrolysis on global model budgets of
640   tropospheric nitrogen oxides, ozone, and OH, Geophys. Res. Lett., 32, 1–4, 2005
641
642   Fairlie, T.D., Jacob, D.J., and Park, R.J.: The impact of transpacific transport of mineral dust in the United States,
643   Atmos. Environ., 41, 6, 1251-1266, doi:10.1016/j.atmosenv.2006.09.048, 2007
644
645   Fischer, E.V., Jacob, D.J., Millet, D.B., Yantosca, R.M.,and Mao, J.: The role of the ocean in the global
646   atmospheric budget of acetone, Geophys. Res. Lett., 39, L01807, doi:10.1029/2011gl050086, 2012
647
648   Fittschen, C., Whalley, L.K., and Heard, D.E.: The reaction of CH_3O_2 radicals with OH radicals: A neglected sink
649   for CH_3O_2 in the remote atmosphere, Environ. Sci. Technol., 118, 7700-7701, 2014
650
651   Fomba, K.W., Muller, K., van Pinxteren, D., Poulain, L., van Pinxteren, M., and Herrmann, H., Long-term
652   chemical characterization of tropical and marine aerosols at the Cape Verde Atmospheric Observatory (CVAO)
653   from 2007 to 2011, Atmos. Chem. Phys., 14, 17, 8883-8904, doi:10.5194/acp-14-8883-2014, 2014
654
655   Fu, T.-M., Jacob, D.J., Wittrock, F., Burrows, J.P., Vrekoussis, M., and Henze, D.K.: Global budgets of
656   atmospheric glyoxal and methylglyoxal, and implications for formation of secondary organic aerosols, J.
657   Geophys. Res., 113, D15303, doi:10.1029/2007jd009505, 2008
658
659   Fuchs, H., Bohn, B., Hofzumahaus, A., Holland, F., Lu, K. D., Nehr, S., Rohrer, F., Wahner, A.: Detection of
660   HO_2 by laser induced fluorescence: calibration and interferences from RO_2 radicals, Atmos. Meas. Tech., 4, 1209–
661   1225, 2011
662
663   George, I.J., Matthews, P.S.J., Whalley, L.K., Brooks, B., Goddard, A., Baeza-Romero, M.T., Heard, D.E.:
664   Measurements of uptake coefficients for heterogeneous loss of HO_2 onto submicron inorganic salt aerosols, Phys.
665   Chem. Chem. Phys., 15, 12829-12845, 2013
666
667   Gomez Martin, J.C., Mahajan, A.S., Hay, T.D., Prados-Roman, C., Ordonez, C., MacDonald, S.M., Plane, J.M.C.,
668   Sorribas, M., Gil, M., Francisco Paredes Mora, J., Agama Reyes, M.V., Oram, D.E., Leedham, E., Saiz-Lopez,
669   A.: Iodine chemistry in the eastern Pacific marine boundary layer, J. Geophys. Res. Atmos., 118, 887-904, 2013
670

Atmospheric
Chemistry
and Physics
Discussions

671 Guenther, A., Karl, T., Harley, P., Wiedinmyer, C., Palmer, P.I., and Geron, C.: Estimates of global terrestrial
672 isoprene emissions using MEGAN (Model of Emissions of Gases and Aerosols from Nature), Atmos. Chem.
673 Phys., 6, 3181-3210, 2006
674
675 Heald, C.L., Coe, H., Jimenez, J.L., Weber, R.J., Bahreini, R., Middlebrook, A.M., Russell, L.M., Jolleys, M.,
676 Fu, T.M., Allan, J.D., Bower, K.N., Capes, G., Crosier, J., Morgan, W.T., Robinson, N.H., Williams, P.I.,
677 Cubison, M.J., De Carlo, P.F., and Dunlea, E.J.: Exploring the vertical profile of atmospheric organic aerosol:
678 comparing 17 aircraft field campaigns with a global model, Atmos. Chem. Phys., 11, 24, 12673-12696,
679 doi:10.5194/acp-11-12673-2011, 2011
680
681 Heard, D. E., Read, K. A., Methven, J., Al-Haider, S., Bloss, W. J., Johnson, G. P., Pilling, M. J., Seakins, P. W.,
682 Smith, S. C., Sommariva, R., Stanton, J. C., Still, T. J., Ingham, T., Brooks, B., De Leeuw, G., Jackson, A. V.,
683 McQuaid, J. B., Morgan, R., Smith, M. H., Carpenter, L. J., Carslaw, N., Hamilton, J., Hopkins, J. R., Lee, J. D.,
684 Lewis, A. C., Purvis, R. M., Wevill, D. J., Brough, N., Green, T., Mills, G., Penkett, S. A., Plane, J. M. C., Saiz-
685 Lopez, A., Worton, D., Monks, P. S., Fleming, Z., Rickard, A. R., Alfarra, M. R., Allan, J. D., Bower, K., Coe,
686 H., Cubison, M., Flynn, M., McFiggans, G., Gallagher, M., Norton, E. G., O'Dowd, C. D., Shillito, J., Topping,
687 D., Vaughan, G., Williams, P., Bitter, M., Ball, S. M., Jones, R. L., Povey, I. M., O'Doherty, S., Simmonds, P.
688 G., Allen, A., Kinnersley, R. P., Beddows, D. C. S., Dall'Osto, M., Harrison, R. M., Donovan, R. J., Heal, M. R.,
689 Jennings, S. G., Noone, C., Spain, G.: The North Atlantic Marine Boundary Layer Experiment (NAMBLEX).
690 Overview of the campaign held at Mace Head, Ireland, in summer 2002, Atmos. Chem. Phys., 6, 2241–2272,
691 doi:10.5194/acp-6-2241-2006, 2006
692
693 Henze, D.K., Hakami, A., and Seinfeld, J.H.: Development of the adjoint of GEOS-Chem, Atmos. Chem. Phys.,
694 7, 9, 2413-2433, 2007
695
696 Henze, D.K., Seinfeld, J.H., and Shindell, D.T.: Inverse modeling and mapping US air quality influences of
697 inorganic PM2.5 precursor emissions using the adjoint of GEOS-Chem, Atmos. Chem. Phys., 9, 16, 5877-5903,
698 2009
699
700 Hoffmann, T., O'Dowd, C.D., and Seinfeld, J.H.: Iodine oxide homogeneous nucleation: An explanation for
701 coastal new particle production, Geophys. Res. Lett., 28, 10, 1949-1952, doi:10.1029/2000GL012399, 2001
702
703 Holmes, C.D., Jacob, D.J., and Yang, X.: Global lifetime of elemental mercury against oxidation by atomic
704 bromine in the free troposphere, Geophys. Res. Lett., 33, L20808, doi:10.1029/2006gl027176, 2006
705
706 Holmes, C.D., Jacob, D.J., Corbitt, E.S., Mao, J., Yang, X., Talbot, R., and Slemr, F.: Global atmospheric model
707 for mercury including oxidation by bromine atoms, Atmos. Chem. Phys., 10, 12037–12057, doi:10.5194/acp-10-
708 12037-2010, 2010
709
710 Hu, L., Jacob, D.J., Liu, X., Zhang, Y., Zhang, L., Kim, P.S., Sulprizio, M.P., and Yantosca, R.M.: Global budget
711 of tropospheric ozone: Evaluating recent model advances with satellite (OMI), aircraft (IAGOS), and ozonesonde
712 observations, Atmos. Environ., doi:10.1016/j.atmosenv.2017.08.036, 2017
713

714   Jacob, D.J.: Heterogeneous chemistry and tropospheric ozone, Atmos. Environ., 34, 2131–2159,
715   doi:10.1016/S1352- 2310(99)00462-8, 2000
716
717   Jacobson, M.Z. and Turco, R.P.: SMVGEAR: A sparse-matrix, vectorized gear code for atmospheric models,
718   Atmos. Environ., 28, 273–284, 1994
719
720   Jaeglé, L., Quinn, P.K., Bates, T.S., Alexander, B., and Lin, J.-T.: Global distribution of sea salt aerosols: new
721   constraints from in situ and remote sensing observations, Atmos. Chem. Phys., 11, 3137–3157, doi:10.5194/acp-
722   11-3137-2011, 2011
723
724   Jenkin, M.E., Saunders, S.M., Wagner, V., Pilling, M.J., Protocol for the development of the Master Chemical
725   Mechanism, MCM v3 (Part B): tropospheric degradation of aromatic volatile organic compounds, Atmos. Chem.
726   Phys., 3, 181–193, 2003
727
728   Kanaya, Y., Matsumoto, J., Kato, S., and Akimoto, H.: Behavior of OH and HO_2 radicals during the Observations
729   at a Remote Island of Okinawa (ORION99) field campaign. 2. Comparison between observations and
730   calculations, J. Geophys. Res.-Atmos., 106, 24209–24223, 2001
731
732   Kanaya, Y., Yokouchi, Y., Matsumoto, J., Nakamura, K., Kato, S., Tanimoto, H., Furutani, H., Toyota, K., and
733   Akimoto, H.: Implications of iodine chemistry for daytime HO_2 levels at Rishiri Island, Geophys. Res. Lett., 29,
734   1212, doi:10.1029/2001GL014061, 2002
735
736   Kanaya, Y., Cao, R., Kato, S., Miyakawa, Y., Kajii, Y., Tanimoto, H., Yokouchi, Y., Mochida, M., Kawamura,
737   K., Akimoto, H.: Chemistry of OH and HO_2 radicals observed at Rishiri Island, Japan, in September 2003:
738   Missing daytime sink of HO_2 and positive nighttime correlations with monoterpenes, J. Geophys. Res.-Atmos.,
739   112, D11308, doi:10.1029/2006JD007987, 2007
740
741   Lakey, P.S.J., George, I.J., Whalley, L.K., Baeza-Romero, M.T., and Heard, D.E.: Measurements of HO_2 update
742   coefficients onto single component organic aerosols, Environ. Sci. Technol., 49, 8, 4878-4885,
743   doi:10.1021/acs.est.5b00948, 2015
744
745   Lee, J.D., Moller, S.J., Read, K.A., Lewis, A.C., Mendes, L., Carpenter, L.J.: Year-round measurements of
746   nitrogen oxides and ozone in the tropical North Atlantic marine boundary layer, J. Geophys. Res., 114, D21302,
747   doi:10.1029/2009JD011878, 2009
748
749   Lee, J. D., McFiggans, G., Allan, J. D., Baker, A. R., Ball, S. M., Benton, A. K., Carpenter, L. J., Commane, R.,
750   Finley, B. D., Evans, M., Fuentes, E., Furneaux, K., Goddard, A., Good, N., Hamilton, J. F., Heard, D. E.,
751   Herrmann, H., Hollingsworth, A., Hopkins, J. R., Ingham, T., Irwin, M., Jones, C. E., Jones, R. L., Keene, W. C.,
752   Lawler, M. J., Lehmann, S., Lewis, A. C., Long, M. S., Mahajan, A., Methven, J., Moller, S. J., Mller, K., Muller,
753   T., Niedermeier, N., O'Doherty, S., Oetjen, H., Plane, J. M. C., Pszenny, A. A. P., Read, K. A., Saiz-Lopez, A.,
754   Saltzman, E. S., Sander, R., von Glasow, R., Whalley, L., Wiedensohler, A., Young, D.: Reactive Halogens in
755   the Marine Boundary Layer (RHaMBLe): the tropical North Atlantic experiments, Atmos. Chem. Phys., 10,
756   1031–1055, 2010

Atmospheric
Chemistry
and Physics
Discussions

757

758 Leser, H., Honninger, G., Platt, U.: MAX-DOAS measurements of BrO and NO_2 in the marine boundary layer,
759 Geophys. Res. Lett., 30, doi:10.1029/2002GL015 811, 2003

760

761 Liao, H., Henze, D.K., Seinfeld, J.H., Wu, S.L., and Mickley, L.J.: Biogenic secondary organic aerosol over the
762 United States: Comparison of climatological simulations with observations, J. Geophys. Res. Atmos., 112, D6,
763 D06201, 1-19, doi:10.1029/2006JD007813, 2007

764

765 Liu, H., Jacob, D.J., Bey, I., and Yantosca, R.M.: Constraints from ^{210}Pb and [7]Be on wet deposition and transport
766 in a global three-dimensional chemical tracer model driven by assimilated meteorological fields, J. Geophys.
767 Res., 106, 12109–12128, doi:10.1029/2000jd900839, 2001

768

769 MacDonald, S.M., Gómez Martín, J.C., Chance, R., Warriner, S., Saiz-Lopez, A., Carpenter, L.J., and Plane,
770 J.M.C.: A laboratory characterisation of inorganic iodine emissions from the sea surface: dependence on oceanic
771 variables and parameterisation for global modelling, Atmos. Chem. Phys., 14, 5841–5852, doi:10.5194/acp-14-
772 5841-2014, 2014

773

774 Mahajan, A.S., Plane, J.M.C., Oetjen, H., Mendes, L., Saunders, R.W., Saiz-Lopez, A., Jones, C.E., Carpenter,
775 L.J., McFiggans, G.B.: Measurement and modelling of tropospheric reactive halogen species over the tropical
776 Atlantic Ocean, Atmos. Chem. Phys., 10, 4611-4624, 2010a

777

778 Mahajan, A.S., Whalley, L.K., Kozlova, E., Oetjen, H., Mendez, L., Furneaux, K.L., Goddard, A., Heard, D.E.,
779 Plane, J.M.C., Saiz-Lopez, A.: DOAS observations of formaldehyde and its impact on the HO_x balance in the
780 tropical Atlantic marine boundary layer, J. Atmos. Chem., 66, 167-178, 2010b

781

782 Mahajan, A. S., Sorribas, M., Gomez Martn, J. C., MacDonald, S. M., Gil, M., Plane, J. M. C., Saiz-Lopez, A.:
783 Concurrent observations of atomic iodine, molecular iodine and ultrafine particles in a coastal environment,
784 Atmos. Chem. Phys., 11, 2545–2555, doi:10.5194/acp-11-2545-2011, 2011

785

786 Mao, J., Jacob, D.J., Evans, M.J., Olson, J.R., Ren, X., Brune, W.H., Clair, J.M. St., Crounse, J.D., Spencer, K.M.,
787 Beaver, M.R., Wennberg, P.O., Cubison, M.J., Jimenez, J.L., Fried, A., Weibring, P., Walega, J.G., Hall, S.R.,
788 Weinheimer, A.J., Cohen, R.C., Chen, G., Crawford, J.H., McNaughton, C., Clarke, A.D., Jaegle, L., Fisher, J.A.,
789 Yantosca, R.M., Le Sager, P., and Carouge, C.: Chemistry of hydrogen oxide radicals (HO_x) in the Arctic
790 troposphere in spring, Atmos. Chem. Phys., 10, 5823–5838, doi:10.5194/acp-10-5823-2010, 2010

791

792 Mao, J., Fan, S., Jacob, D.J., Travis, K.R.: Radical loss in the atmosphere from Cu-Fe redox coupling in aerosols,
793 Atmos. Chem. Phys., 13, 509-519, 2013

794

795 Matthews, P.S.J., Baeza-Romero, M.T., Whalley, L.K., and Heard, D.E.: Uptake of HO_2 radicals onto Arizona
796 test dust particles using an aerosol flow tube, Atmos. Chem. Phys., 14, 7397-7408, doi:10.5194/acp-14-7397-
797 2014, 2014

798

Atmospheric
Chemistry
and Physics
Discussions

799   McFiggans, G., Coe, H., Burgess, R., Allan, J., Cubison, M., Alfarra, M. R., Saunders, R., Saiz-Lopez, A., Plane,
800   J. M. C., Wevill, D., Carpenter, L., Rickard, A. R., Monks, P. S.: Direct evidence for coastal iodine particles from
801   *Laminaria* macroalgae – linkage to emissions of molecular iodine, Atmos. Chem. Phys., 4, 701–713,
802   doi:10.5194/acp-4-701-2004, 2004

804   McFiggans, G., Bale, C. S. E., Ball, S. M., Beames, J. M., Bloss, W.J., Carpenter, L. J., Dorsey, J., Dunk, R.,
805   Flynn, M. J., Furneaux, K. L., Gallagher, M. W., Heard, D. E., Hollingsworth, A. M., Hornsby, K., Ingham, T.,
806   Jones, C. E., Jones, R. L., Kramer, L. J., Langridge, J. M., Leblanc, C., LeCrane, J.-P., Lee, J. D., Leigh, R. J.,
807   Longley, I., Mahajan, A. S., Monks, P. S., Oetjen, H., Orr-Ewing, A. J., Plane, J. M. C., Potin, P., Shillings, A. J.
808   L., Thomas, F., von Glasow, R., Wada, R., Whalley, L. K., Whitehead, J. D.: Iodine-mediated coastal particle
809   formation: an overview of the Reactive Halogens in the Marine Boundary Layer (RHaMBLe) Roscoff coastal
810   study, Atmos. Chem. Phys., 10, 2975–2999, doi:10.5194/acp-10-2975-2010, 2010

812   McLinden, C.A., Olsen, S.C., Hannegan, B., Wild, O., Prather, M.J., and Sundet, J.: Stratospheric ozone in 3-D
813   models: A simple chemistry and the cross-tropopause flux, J. Geophys. Res., 105, 14653–14665, 2000

815   Millet, D.B., Bassandorj, M., Farmer, D.K., Thornton, J.A., Baumann, K., Brophy, P., Chaliyakunnel, S., de
816   Gouw, J.A., Graus, M., Hu, L., Koss, A., Lee, B.H., Lopez-Hilfiker, F.D., Neuman, J.A., Paulot, F., Peischl, J.,
817   Pollack, I.B., Ryerson, T.B., Warneke, C., Williams, B.J., and Xu, J.: A large and ubiquitous source of
818   atmospheric formic acid, Atmos. Chem. Phys., 15, 6283-6304, doi:10.5194/acp-15-6283-2015, 2015

820   Muller, K., Lehmann, S., van Pinxteren, D., Gnauk, T., Niedermeier, N., Wiedensohler, A., Herrmann, H.: Particle
821   characterization at the Cape Verde atmospheric observatory during the 2007 RHaMBLe intensive, Atmos. Chem.
822   Phys., 10, 2709-2721, 2010

824   Murray, L.T., Jacob, D.J., Logan, J.A., Hudman, R.C., and Koshak, W.J.: Optimized regional and interannual
825   variability of lightning in a global chemical transport model constrained by LIS/OTD satellite data, J. Geophys.
826   Res. Atmos., 117, D20307, doi:10.1029/2012JD017934, 2012

828   Nassar, R., Logan, J. A., Megretskaia, I. A., Murray, L. T., Zhang, L., and Jones, D. B. A.: Analysis of tropical
829   tropospheric ozone, carbon monoxide, and water vapour during the 2006 El Nino using TES observations and the
830   GEOS-Chem model, J. Geophys. Res., 114, D17304, doi:10.1029/2009JD011760, 2009

832   NOAA CMDL flask analysis, ftp://ftp.cmdl.noaa.gov/ccg/ch4/, GLOBALVIEW-CH4, 2010-2011: Cooperative
833   Atmospheric Data Integration Project – Methane. CD-ROM, NOAA ESRL, Boulder, Colorado, also available on
834   Internet via anonymous FTP to ftp://ftp.cmdl.noaa.gov/ccg/ch4/, path: ccg/CH4/GLOBALVIEW, 2009, access:
835   17 Feb 2010

837   Novelli, P.C., Lang, P.M., Masarie, K.A., Hurst, D.F., Myers, R., Elkins, J.W.: Molecular hydrogen in the
838   troposphere: Global distribution and budget, J. Geophys. Res., 104, D23, 30,427-30,444, 1999

840   O'Dowd, C.D. and Hoffmann, T.: Coastal new particle formation: a review of the current state-of-the-art, Environ.
841   Chem., 2, 245, doi:10.1071/EN05077, 2005

Atmospheric
Chemistry
and Physics
Discussions

842

843 Olivier, J.G.J., and Peters, J.A.H.W.: CO_2 from non-energy use of fuels: A global, regional and national
844 perspective based on the IPCC Tier 1 approach, Res. Conserv., Recycl., 45, 3, 210-225,
845 doi:10.1016/j.resconrec.2005.05.008, 2005

846

847 Ordonez, C., Lamarque, J.-F., Tilmes, S., Kinnison, D.E., Atlas, E.L., Blake, D.R., Sousa Santos, G., Brasseur,
848 G., Saiz-Lopez, A.: Bromine and iodine chemistry in a global chemistry-climate model: description and
849 evaluation of very short-lived oceanic sources, Atmos. Chem. Phys., 12, 1423-1447, 2012

850

851 Park, R.J., Jacob, D.J., Field, B.D., Yantosca, R.M., and Chin, M.: Natural and transboundary pollution influences
852 on sulfate-nitrate-ammonium aerosols in the United States: Implications for policy, J. Geophys. Res. Atmos., 109,
853 D15204, doi:10.1029/2003JD004473, 2004

854

855 Parrella, J.P., Jacob, D.J., Liang, Q., Zhang, Y., Mickley, L.J., Miller, B., Evans, M.J., Yang, X., Pyle, J.A., Theys,
856 N., Van Roozendael, M.: Tropospheric bromine chemistry: implications for present and pre-industrial ozone and
857 mercury, Atmos. Chem. Phys., 12, 6723-6740, 2012

858

859 Paulot, F., Crounse, J.D., Kjaergaard, H.G., Kürten, A., St. Clair, J.M., Seinfeld, J.H., and Wennberg, P.O.:
860 Unexpected Epoxide Formation in the Gas-Phase Photooxidation of Isoprene, Science, 325, 730–733, 2009

861

862 Peters, C., Pechtl, S., Stutz, J., Hebestreit, K., Honninger, G., Heumann, K. G., Schwarz, A., Winterlik, J., and
863 Platt, U.: Reactive and organic halogen species in three different European coastal environments, Atmos. Chem.
864 Phys., 5, 3357–3375, doi:10.5194/acp-5-3357-2005, 2005

865

866 Pye, H.O.T., Liao, H., Wu, S., Mickley, L.J., Jacob, D.J., Henze, D.K., and Seinfeld, J.H.: Effect of changes in
867 climate and emissions on future sulfate-nitrate-ammonium aerosol levels in the United States, J. Geophys. Res.
868 Atmos., 114, D01205, doi:10.1029/2008JD010701, 2009

869

870 Read, K. A., Mahajan, A. S., Carpenter, L. J., Evans, M. J., Faria, B. V. E., Heard, D. E., Hopkins, J. R., Lee, J.
871 D., Moller, S. J., Lewis, A. C., Mendes, L., McQuaid, J. B., Oetjen, H., Saiz-Lopez, A., Pilling, M. J., Plane, J.
872 M. C.: Extensive halogen mediated ozone destruction over the tropical Atlantic Ocean, Nature, 453, 7199, 1232–
873 1235, 2008

874

875 Saiz-Lopez, A. and Plane, J. M. C.: Novel iodine chemistry in the marine boundary layer, Geophys. Res. Lett.,
876 31, L04112, doi:10.1029/2003GL019215, 2004

877

878 Saiz-Lopez, A., Plane, J. M. C., Shillito, J. A.: Bromine oxide in the mid-latitude marine boundary layer, Geophys.
879 Res. Lett., 31, L03111, doi:10.1029/2003GL018956, 2004

880

881 Saiz-Lopez, A., Shillto, J.A., Coe, H., Plane, J.M.C.: Measurements and modelling of I_2, IO, OIO, BrO and NO_3
882 in the mid-latitude marine boundary layer, Atmos. Chem. Phys., 6, 1513-1528, 2006

883

884 Saiz-Lopez, A., Lamarque, J.-F., Kinnison, D.E., Tilmes, S., Ordonez, C., Orlando, J.J., Conley, A.J., Plane,
885 J.M.C., Mahajan, A.S., Sousa Santos, G., Atlas, E.L., Blake, D.R., Sander, S.P., Schauffler, S., Thompson, A.M.,
886 Brasseur, G.: Estimating the climate significance of halogen-driven ozone loss in the tropical marine troposphere,
887 Atmos. Chem. Phys., 12, 3939-3949, 2012
888
889 Saiz-Lopez, A., von Glasow, R.: Reactive halogen chemistry in the troposphere, Chem. Soc. Rev., 41, 6448-6472,
890 2012
891
892 Sander, R., Keene, W. C., Pszenny, A. A. P., Arimoto, R., Ayers, G. P., Baboukas, E., Cainey, J. M., Crutzen, P.
893 J., Duce, R. A., Honninger, G., Huebert, B. J., Maenhaut, W., Mihalopoulos, N., Turekian, V. C., Van Dingenen,
894 R.: Inorganic bromine in the marine boundary layer: a critical review, Atmos. Chem. Phys., 3, 1301–1336,
895 doi:10.5194/acp-3-1301-2003, 2003
896
897 Sander, S.P., Friedl, R.R., Abbatt, J.P.D., Barker, J.R., Burkholder, J.B., Golden, D.M., Kolb, C.E., Kurylo, M.J.,
898 Moortgat, G.K., Wine, P., Huie, R.E., and Orkin, V.L.: Chemical kinetics and photochemical data for use in
899 atmospheric studies, Evaluation Number 17, Tech. rep., NASA Jet Propulsion Laboratory, Pasadena, 2011
900
901 Sandu, A., Sander, R.: Technical note: Simulating chemical systems in Fortran90 and Matlab with the Kinetic
902 PreProcessor KPP-2.1, Atmos. Chem. Phys., 6, 187-195, 2006
903
904 Saunders, S.M., Jenkin, M.E., Derwent, R.G., Pilling, M.J.: Protocol for the development of the Master Chemical
905 Mechanism, MCM v3 (Part A): tropospheric degradation of non-aromatic volatile organic compounds, Atmos.
906 Chem. Phys., 3, 161-180, 2003
907
908 Schmidt, J.A., Jacob, D.J., Horowitz, H.M., Hu, L., Sherwen, T., Evans, M.J., Liang, Q., Suleiman, R.M., Oram,
909 D.E., Breton, M.L., Percival, C.J., Wang, S., Dix, B., and Volkamer, R.: Modeling the observed tropospheric BrO
910 background: Importance of multiphase chemistry and implications for ozone, OH, and mercury, J. Geophys. Res.
911 Atmos., 121, 19, 11819-11835, doi:10.1002/2015JD024229, 2016
912
913 Schwarz, S. E.: Mass-transport considerations pertinent to aqueous phase reactions of gases in liquid-water
914 clouds, Chemistry of Multiphase Atmospheric Systems, NATO ASI Series, G6, Jaeschke ed., Springer-Verlag,
915 Berlin, 415–471, 1986
916
917 Sherwen, T., Evans, M.J., Carpenter, L.J., Andrews, S.J., Lidster, R.T., Dix, B., Koenig, T.K., Sinreich, R.,
918 Ortega, I., Volkamer, R., Saiz-Lopez, A., Prados-Roman, C., Mahajan, A. S., and Ordóñez, C.: Iodine's impact
919 on tropospheric oxidants: a global model study in GEOS-Chem, Atmos. Chem. Phys., 16, 1161– 1186,
920 doi:10.5194/acp-16-1161-2016, 2016a
921
922 Sherwen, T., Schmidt, J.A., Evans, M.J., Carpenter, L.J., Groβmann, K., Eastham, S.D., Jacob, D.J., Dix, B.,
923 Koenig, T.K., Sinreich, R., Ortega, I., Volkamer, R., Saiz-Lopez, A., Prados-Roman, C., Mahajan, A.S., and
924 Ordóñez, C.: Global impacts of tropospheric halogens (Cl, Br, I) on oxidants and composition in GEOS-Chem,
925 Atmos. Chem. Phys., 16, 12239-12271, doi:10.5194/acp-16-12239-2016, 2016b
926

927   Sherwen, T.M., Evans, M.J., Spracklen, D.V., Carpenter, L.J., Chance, R., Baker, A.R., Schmidt, J.A., and
928   Breider, T.J.: Global modeling of tropospheric iodine aerosol, Geophys, Res. Lett., 43, 18, 19912-10019,
929   doi:1002/2016GL070062, 2016c

931   Sherwen, T., Evans, M.J., Carpenter, L.J., Schmidt, J.A., and Mickley, L.J.: Halogen chemistry reduces
932   tropospheric O_3 radiative forcing, Atmos. Chem. Phys., 17, 1557-1569, doi:10.5194/acp-17-1557-2017, 2017

934   Simpson, W.R., Brown, S.S., Saiz-Lopez, A., Thornton, J.A., and von Glasow, R.: Tropospheric Halogen
935   Chemistry: Sources, Cycling, and Impacts, Chem. Rev., 115, 4035–4062, doi:10.1021/cr5006638, 2015

937   Smith, S. C., Lee, J. D., Bloss, W. J., Johnson, G. P., Ingham, T., Heard, D. E.: Concentrations of OH and HO_2
938   radicals during NAMBLEX: measurements and steady state analysis, Atmos. Chem. Phys., 6, 1435–1453, 2006

940   Sommariva, R., Bloss, W.J., Brough, N., Carslaw, N., Flynn, M., Haggerstone, A.-L., Heard, D.E., Hopkins, J.R.,
941   Lee, J.D., Lewis, A.C., McFiggans, G., Monks, P.S., Penkett, S.A., Pilling, M.J., Plane, J.M.C., Read, K.A., Saiz-
942   Lopez, A., Rickard, A.R., Williams, P.I.: OH and HO_2 chemistry during NAMBLEX: role of oxygenates, halogen
943   oxides and heterogeneous uptake, Atmos. Chem. Phys., 6, 1135-1153, 2006

945   Sommariva, R., Pilling, M.J., Bloss, W.J., Heard, D.E., Lee, J.D., Fleming, Z.L., Monks, P.S., Plane, J.M.C.,
946   Saiz-Lopez, A., Ball, S.M., Bitter, M., Jones, R.L., Brough, N., Penkett, S.A., Hopkins, J.R., Lewis, A.C., Read,
947   K.A.: Night-time radical chemistry during the NAMBLEX campaign, Atmos. Chem. Phys., 7, 587-598, 2007

949   Stone, D., Evans, M.J., Commane, R., Ingham, T., Floquet, C.F.A., McQuaid, J.B., Brookes, D.M., Monks, P.S.,
950   Purvis, R., Hamilton, J.F., Hopkins, J., Lee, J., Lewis, A.C., Stewart, D., Murphy, J.G., Mills, G., Oram, D.,
951   Reeves, C.E., Heard, D.E. : HO_x observations over West Africa during AMMA: Impact of isoprene and NO_x,
952   Atmos. Chem. Phys., 10, 9415-9429, 2010

954   Stone, D., Evans, M.J., Edwards, P.M., Commane, R., Ingham, T., Rickard, A.R., Brookes, D.M., Hopkins, J.,
955   Leigh, R.J., Lewis, A.C., Monks, A.C., Monks, P.S., Oram, D., Reeves, C.E., Stewart, D., Heard, D.E.: Isoprene
956   oxidation mechanisms: measurements and modelling of OH and HO_2 over a South-East Asian tropical rainforest
957   during the OP3 field campaign, Atmos. Chem. Phys., 11, 6749-6771, 2011

959   Stone, D., Whalley, L.K., Heard, D.E.: Tropospheric OH and HO_2 radicals: Field measurements and model
960   comparisons, Chem. Soc. Rev., 41, 6348-6404, 2012

962   Stone, D., Evans, M.J., Walker, H., Ingham, T., Vaughan, S., Ouyang, B., Kennedy, O.J., McLeod, M.W., Jones,
963   R.L., Hopkins, J., Punjabi, S., Lidster, R., Hamilton, J.F., Lee, J.D., Lewis, A.C., Carpenter, L.J., Forster, G.,
964   Oram, D..E., Reeves, C.E., Bauguitte, S., Morgan, W., Coe, H., Aruffo, E., Dari-Salisburgo, C., Giammaria, F.,
965   Di Carlo, P., and Heard, D.E.: Radical Chemistry at Night: Comparisons between observed and modeled HO_x,
966   NO_3 and N_2O_5 during the RONOCO project, Atmos. Chem. Phys., 14, 1299-1321, 2014, doi:10.5194/acp-14-
967   1299-2014

968

Atmospheric
Chemistry
and Physics
Discussions

969 Taketani, F., Kanaya, Y., Akimoto, H.: Kinetics of heterogeneous reactions of HO_2 radical at ambient
970 concentration levels with $(NH_4)_2SO_4$ and NaCl aerosol particles, J. Phys. Chem. A., 112, 11, 2370-2377, 2008

972 Theys, N., Van Roozendael, M., Hendrick, F., Yang, X., De Smedt, I., Richter, A., Begoin, M., Errera, Q.,
973 Johnston, P.V., Kreher, K., and De Mazière, M.: Global observations of tropospheric BrO columns using GOME-
974 2 satellite data, Atmos. Chem. Phys., 11, 1791–1811, doi:10.5194/acp-11-1791-2011, 2011

976 Thornton, J.A., Jaegle, L., and McNeill, V.F.: Assessing known pathways for HO_2 loss in aqueous atmospheric
977 aerosols: Regional and global impacts on tropospheric oxidants, J. Geophys. Res. Atmos., 113, D5, D05303, 1-
978 16, doi:10.1029/2007JD009236, 2008

980 van het Bolscher, M., REanalysis of the TROpospheric chemical composition over the past 40 years: A long-term
981 global modeling study of tropospheric chemistry funded under the 5th EU framework programme, *Rep. EU-*
982 *Contract No. EVK2-CT-2002-00170*, 1-77, MPI for Meteorology, Hamburg, Germany

984 Vaughan, S., Ingham, T., Whalley, L.K., Stone, D., Evans, M.J., Read, K.A., Lee, J.D., Moller, S.J., Carpenter,
985 L.J., Lewis, A.C., Fleming, Z.L., Heard, D.E.: Seasonal observations of OH and HO_2 in the remote tropical marine
986 boundary later, Atmos. Chem. Phys., 12, 2149-2172, 2012

988 Vogt, R., Crutzen, P., and Sander, R.: A mechanism for halogen release from sea-salt aerosol in the remote marine
989 boundary layer, Nature, 383, 327–330, 1996

991 Vogt, R., Sander, R., von Glasow, R., and Crutzen, P. J.: Iodine chemistry and its role in halogen activation and
992 ozone loss in the marine boundary layer: A model study, J. Atmos. Chem., 32, 375–395, 1999

994 Volkamer, R., Baidar, S., Campos, T.L., Coburn, S., DiGangi, J.P., Dix, B., Eloranta, E.W., Koenig, T.K., Morley,
995 B., Ortega, I., Pierce, B.R., Reeves, M., Sinreich, R., Wang, S., Zondlo, M.A., and Romashkin, P.A.: Aircraft
996 measurements of BrO, IO, glyoxal, NO_2, H_2O, O_2-O_2 and aerosol extinction profiles in the tropics: comparison
997 with aircraft-/ship-based in situ and lidar measurements, Atmos. Meas. Tech., 8, 2121–2148, doi:10.5194/amt-8-
998 2121-2015, 2015

000 von Glasow, R., von Kuhlmann, R., Lawrence, M. G., Platt, U., Crutzen, P. J.: Impact of reactive bromine
001 chemistry in the troposphere, Atmos. Chem. Phys., 4, 2481–2497, 2004

003 Wang, Y., Jacob, D.J., and Logan, J.A.: Global simulation of tropospheric O_3-NO_x-hydrocarbon chemistry 1.
004 Model formulation, J. Geophys. Res., 103, 10713–10725, doi:10.1029/98jd00158, 1998

006 Wang, Q., Jacob, D.J., Fisher, J.A., Mao, J., Leibensperger, E.M., Carouge, C.C., Le Sager, P., Kondo, Y.,
007 Jimenez, J.L., Cubison, M.J., and Doherty, S.J.: Sources of carbonaceous aerosols and deposited black carbon in
008 the Arctic in winter-spring: implications for radiative forcing, Atmos. Chem. Phys., 11, 23, 12453-12473,
009 doi:10.5194/acp-11-12453-2011, 2011

Atmospheric
Chemistry
and Physics
Discussions

011   Wang, S.-Y., Schmidtd, J., Baidar, S., Coburn, S., Dix, B., Koenig, T., Apel, E., Bowdalo, D., Campos, T.,
012   Eloranta, E., Evans, M., DiGangii, J., Zondlo, M., Gao, R.-S., Haggerty, J., Hall, S., Hornbrook, R., Jacob, D.,
013   Morley, B., Pierce, B., Reeves, M., Romashkin, P., ter Schure, A., and Volkamer, R.: Active and widespread
014   halogen chemistry in the tropical and subtropical free troposphere, P. Natl. Acad. Sci. USA, 112, 9281–9286,
015   doi:10.1073/pnas.1505142112, 2015
016
017   Wesely, M.L.: Parameterization of surface resistance to gaseous dry deposition in regional-scale numerical
018   models, Atmos. Environ., 23, 1293–1304, 1989
019
020   Whalley, L. K., Furneaux, K. L., Gravestock, T., Atkinson, H. M., Bale, C. S. E., Ingham, T., Bloss, W. J., Heard,
021   D. E.: Detection of iodine monoxide radicals in the marine boundary layer using laser induced fluorescence
022   spectroscopy, J. Atmos. Chem., 58(1), 19–39, 2007
023
024   Whalley, L.K., Furneaux, K.L., Goddard, A., Lee, J.D., Mahajan, A., Oetjen, H., Read, K.A., Kaaden, N.,
025   Carpenter, L.J., Lewis, A.C., Plane, J.M.C., Saltzman, E.S., Wiedensohler, A., Heard, D.E.: The chemistry of OH
026   and HO_2 radicals in the boundary layer over the tropical Atlantic Ocean, Atmos. Chem. Phys., 10, 1555-1576,
027   2010
028
029   Whalley, L.K., Blitz, M.A., Desservettaz, M., Seakins, P.W., and Heard, D.E.: Reporting the sensitivity of laser-
030   induced fluorescence instruments used for HO_2 detection to an interference from RO_2 radicals and introducing a
031   novel approach that enables HO_2 and certain RO_2 types to be selectively measured, Atmos. Meas. Tech., 6, 3425-
032   3440, 2013, doi:10.5194/amt-6-3425-2013
033
034   Wild, O., Zhu, X., and Prather, M.J.: Fast-J: Accurate Simulation of In- and Below-Cloud Photolysis in
035   Tropospheric Chemical Models, J. Atmos. Chem., 37, 245–282, doi:10.1023/a:1006415919030, 2000
036
037   Yan, C., Kocevska, S., and Krasnoperov, L.N.: Kinetics of the reaction of CH_3O_2 radicals with OH studied over
038   the 292-526 K temperature range, J. Phys. Chem. A, 120, 6111-6121, 2016
039
040   Yang, X., Cox, R. A., Warwick, N. J., Pyle, J. A., Carver, G. D., O'Connor, F. M., Savage, N. H.: Tropospheric
041   bromine chemistry and its impacts on ozone: A model study, J. Geophys. Res., 110, D23311,
042   doi:10.1029/2005JD006244, 2005
043
044   Zhang, L., Jacob, D.J., Liu, X., Logan, J.A., Chance, K., Eldering, A., and Bojkov, B.R.: Intercomparison methods
045   for satellite measurements of atmospheric composition: application to tropospheric ozone from TES and OMI,
046   Atmos. Chem. Phys., 10, 4725–4739, doi:10.5194/acp-10-4725-2010, 2010
047
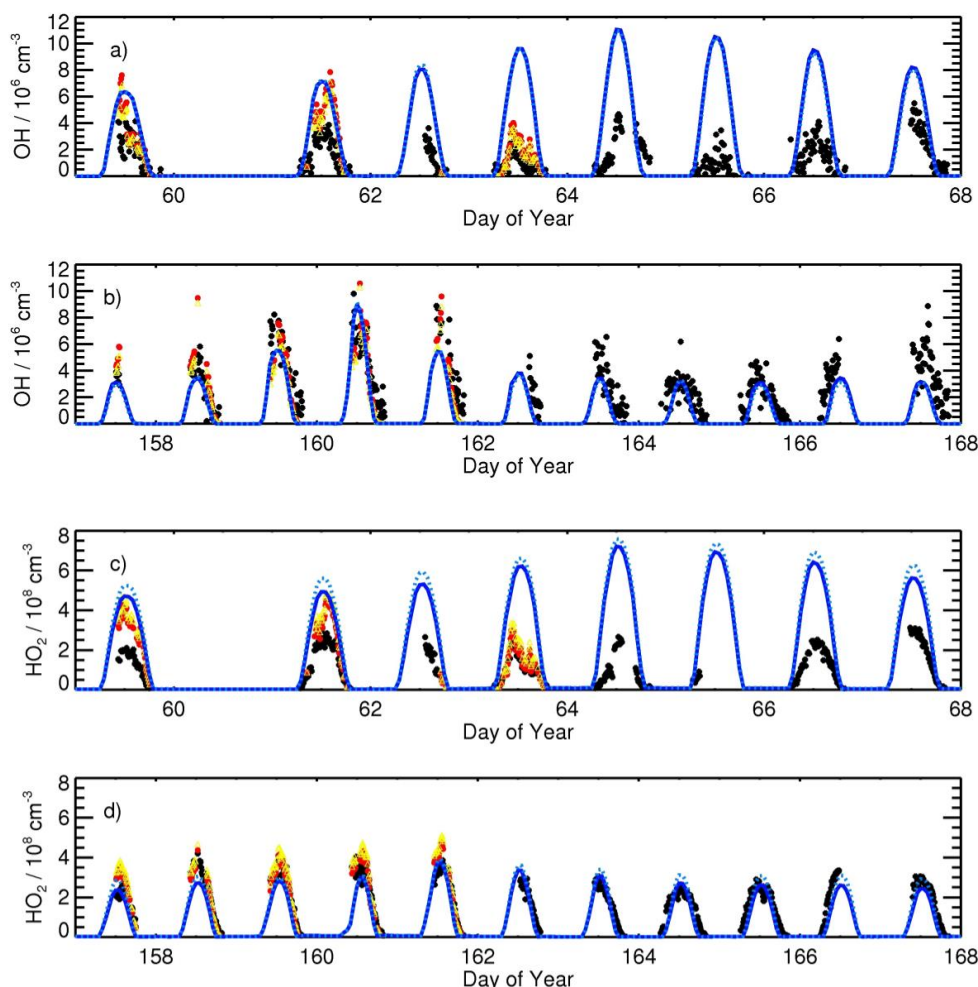
Figures

Figure 1: Observed and modelled concentrations of a) OH during SOS1 (February-March 2009, days 58-68); b) OH during SOS2 (May-June 2009, days 157-168); c) HO$_2$ during SOS1; d) HO$_2$ during SOS2. Observed data are shown in black; box model concentrations with halogen chemistry are shown by filled red circles; box model concentrations without halogen chemistry are shown by open orange triangles; global model concentrations with halogen chemistry are shown by solid dark blue lines; global model concentrations without halogen chemistry are shown by broken blue lines.
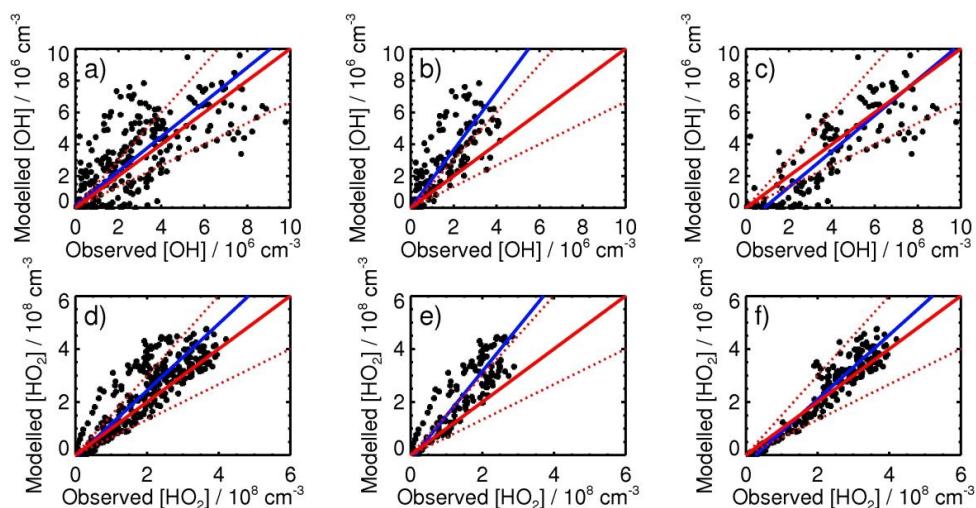
058

059   Figure 2: Comparison of modelled and observed concentrations of a) OH during SOS1 (February-March 2009)

060   and SOS2 (May-June 2009); b) OH during SOS1; c) OH during SOS2; d) HO$_2$ during SOS1 and SOS2; e) HO$_2$

061   during SOS1; f) HO$_2$ during SOS2. In each plot, the solid red line indicates the 1:1 line, with 50 % limits given

062   by the broken red lines. The best fit lines are shown in blue and are described by a) [OH]$_{mod}$ = (1.09 ± 0.11) ×

063   [OH]$_{obs}$ + (0.13 ± 0.38) × 10^6 (r^2 = 0.49); b) [OH]$_{mod}$ = (1.82 ± 0.26) × [OH]$_{obs}$ - (0.01 ± 0.51) × 10^6 (r^2 = 0.56);

064   c) [OH]$_{mod}$ = (1.11 ± 0.15) × [OH]$_{obs}$ - (0.95 ± 0.66) × 10^6 (r^2 = 0.64); d) [HO$_2$]$_{mod}$ = (1.26 ± 0.10) × [HO$_2$]$_{obs}$ -

065   (0.08 ± 0.22) × 10^8 (r^2 = 0.77); e) [HO$_2$]$_{mod}$ = (1.66 ± 0.21) × [HO$_2$]$_{obs}$ - (0.17 ± 0.34) × 10^8 (r^2 = 0.78); f) [HO$_2$]$_{mod}$

066   = (1.21 ± 0.12) × [HO$_2$]$_{obs}$ - (0.32 ± 0.30) × 10^8 (r^2 = 0.91).

067

Atmospheric
Chemistry
and Physics
Discussions

068
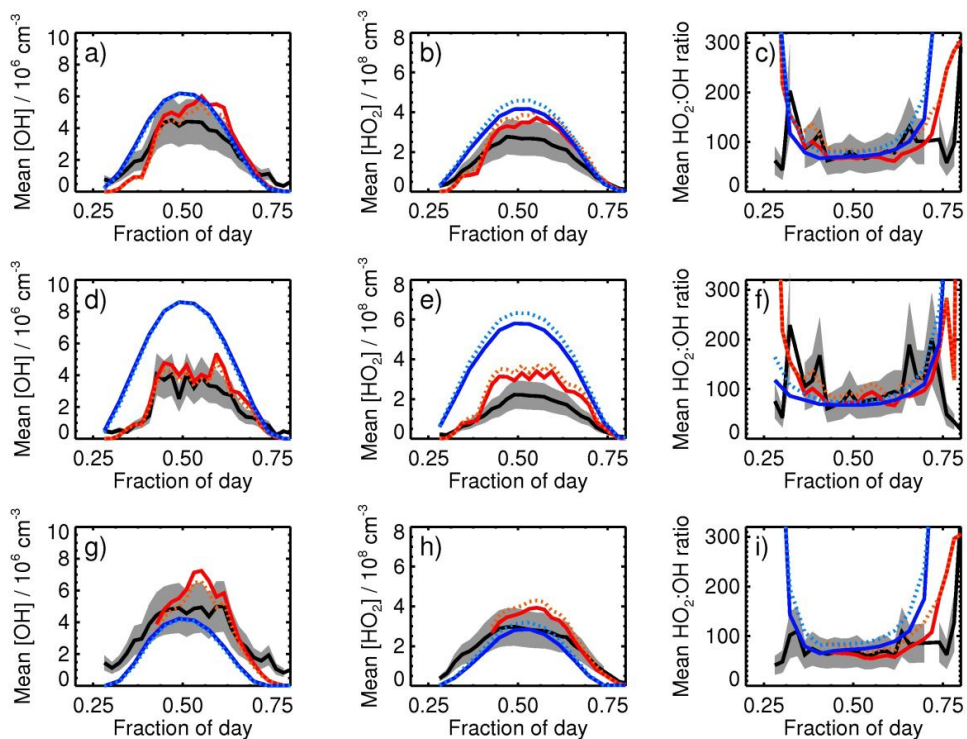
Figure 3: Average diurnal profiles during the Seasonal Oxidant Study (SOS) at the Cape Verde Atmospheric
Observatory for a) OH during both measurement periods; b) HO_2 during both measurement periods; c) HO_2:OH
ratio during both measurement periods; d) OH during SOS1 (Feb-Mar 2009); e) HO_2 during SOS1; f) HO_2:OH
during SOS1; g) OH during SOS2 (May-June); h) HO_2 during SOS2; i) HO_2:OH ratio during SOS2. Observed
data are shown in black, with grey shading indicating the variability in the observations; box model output with
halogen chemistry is shown by solid red lines; box model output without halogen chemistry is shown by broken
orange lines; global model output with halogen chemistry is shown by solid dark blue lines; global model output
without halogen chemistry is shown by broken blue lines.

077

078
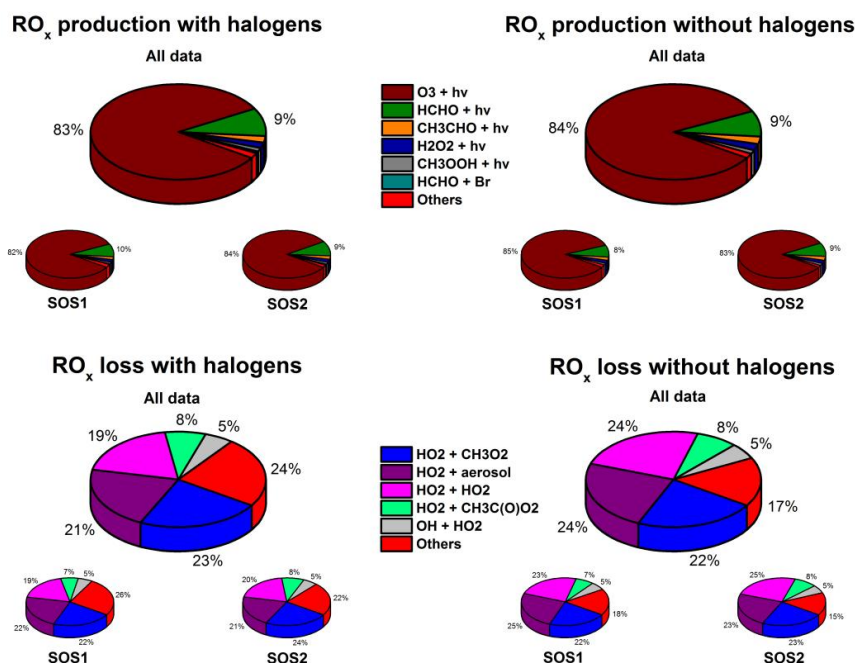
Figure 4: Processes controlling the a) instantaneous RO_x radical production (with RO_x defined here as $OH+HO_2+HOBr+HOI+RO+RO_2$ owing to the rapid processing between HO_2 and $HOBr/HOI$) around noon (1100-1300 hours) for box model simulations with halogen chemistry; b) the instantaneous RO_x radical production around noon for box model simulations without halogen chemistry; c) the instantaneous RO_x radical loss around noon for box model simulations with halogen chemistry; d) the instantaneous RO_x radical loss around noon for box model simulations without halogen chemistry. The main charts show the average results for SOS1+SOS2, with results for SOS1 and SOS2 shown separately in the inset charts.

086
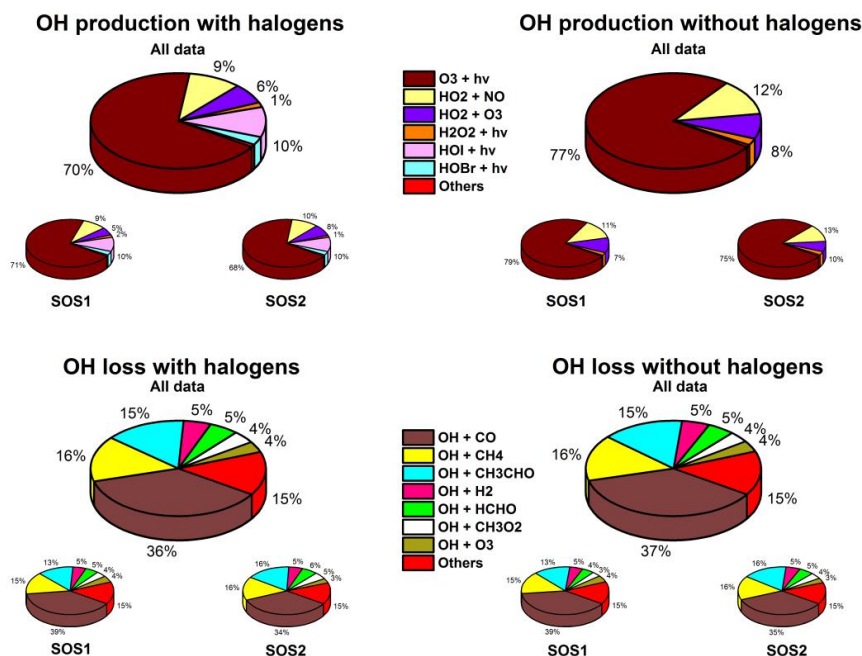
Figure 5: Processes controlling the a) instantaneous OH radical production around noon (1100-1300 hours) for
box model simulations with halogen chemistry; b) the instantaneous OH radical production around noon for box
model simulations without halogen chemistry; c) the instantaneous OH radical loss around noon for box model
simulations with halogen chemistry; d) the instantaneous OH radical loss around noon for box model simulations
without halogen chemistry. The main charts show the average results for SOS1+SOS2, with results for SOS1
and SOS2 shown separately in the inset charts.

093
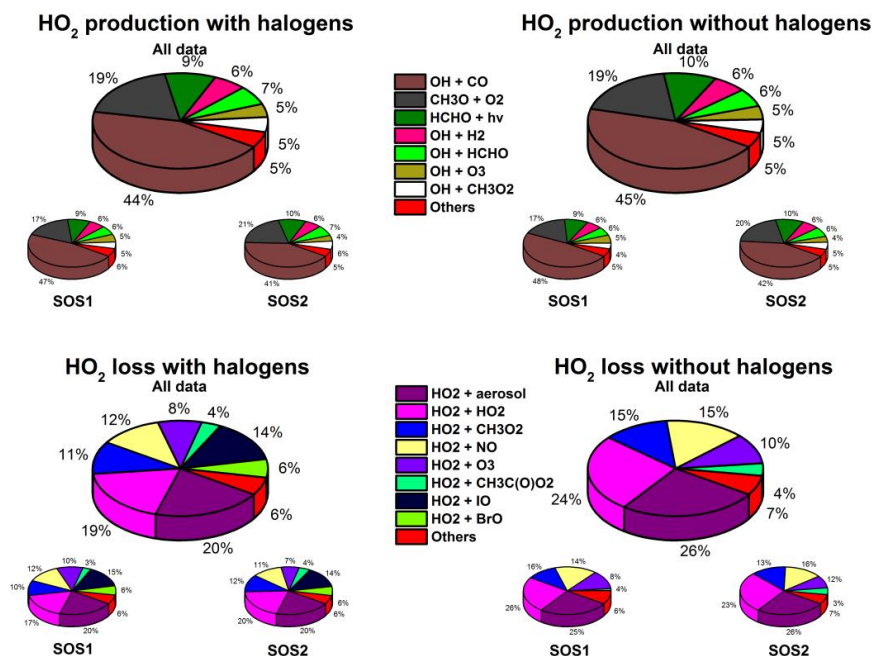
Figure 6: Processes controlling the a) instantaneous HO₂ radical production around noon (1100-1300 hours) for box model simulations with halogen chemistry; b) the instantaneous HO₂ radical production around noon for box model simulations without halogen chemistry; c) the instantaneous HO₂ radical loss around noon for box model simulations with halogen chemistry; d) the instantaneous HO₂ radical loss around noon for box model simulations without halogen chemistry. The main charts show the average results for SOS1+SOS2, with results for SOS1 and SOS2 shown separately in the inset charts.

100

Atmospheric
Chemistry
and Physics
Discussions

Open Access

101

102
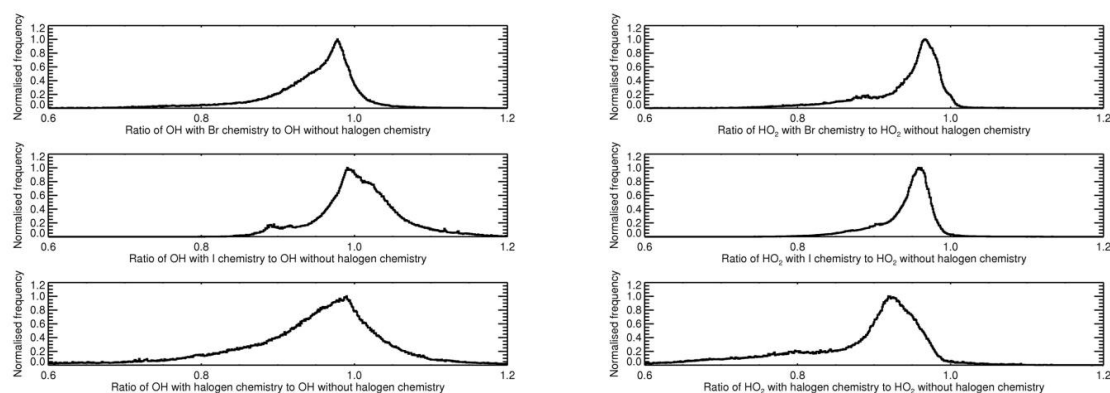
103

104 Figure 7: Normalised probability distribution functions showing the fractional changes in OH (left hand side) and

105 HO$_2$ (right hand side) in GEOS-Chem for all grid boxes on inclusion of bromine chemistry (upper panels), iodine

106 chemistry (middle panels) and bromine and iodine chemistry combined (lower panels).

107
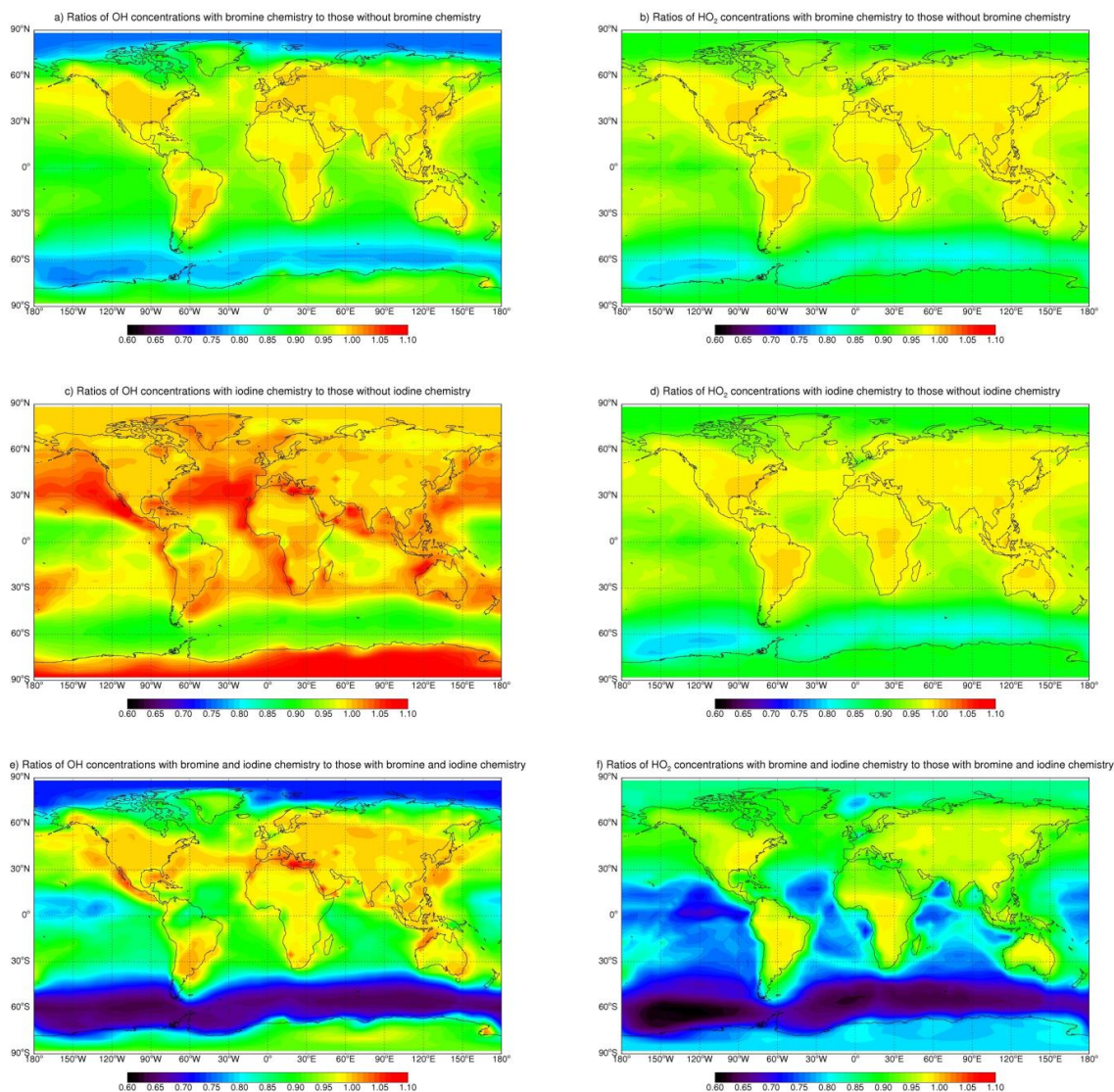
Figure 8: Percentage changes to annual surface layer concentrations of OH (left hand side) and HO_2 (right hand side) in GEOS-Chem on inclusion of bromine chemistry (upper panels), iodine chemistry (middle panels) and bromine and iodine chemistry combined (lower panels).

111
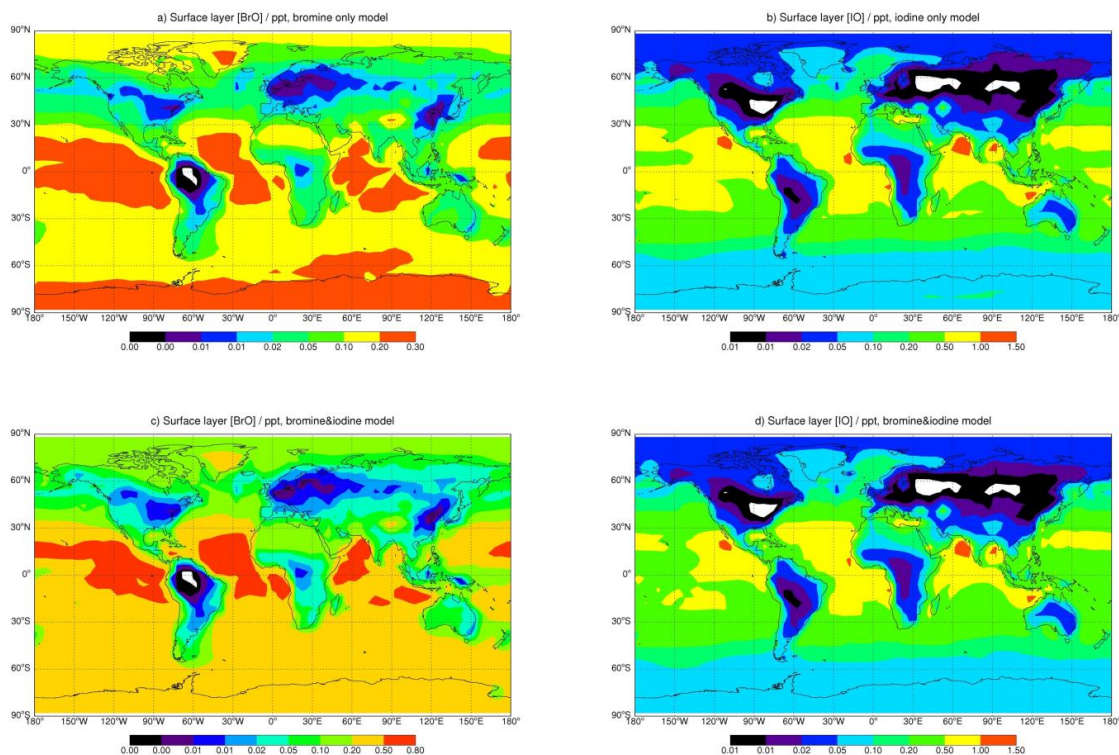
Figure 9: Annual surface layer mixing ratios (ppt) of BrO and IO radicals in GEOS-Chem for model runs with
just bromine chemistry (upper left panel), just iodine chemistry (upper right panel) and bromine and iodine
chemistry combined (lower panels).

115

116

117